AD-A125 640 THE EFFECTS OF SMALL DEFORMATION ON CREEP AND STRESS RUPTURE BEHAVIOR OF.. (U) HENRY KRUMB SCHOOL OF MINES NEW YORK V C NARDONE ET AL. 07 JAN 83 AFOSR-TR-83-0095 1/1

UNCLASSIFIED AFOSR-78-3637 F/G 11/6 NL

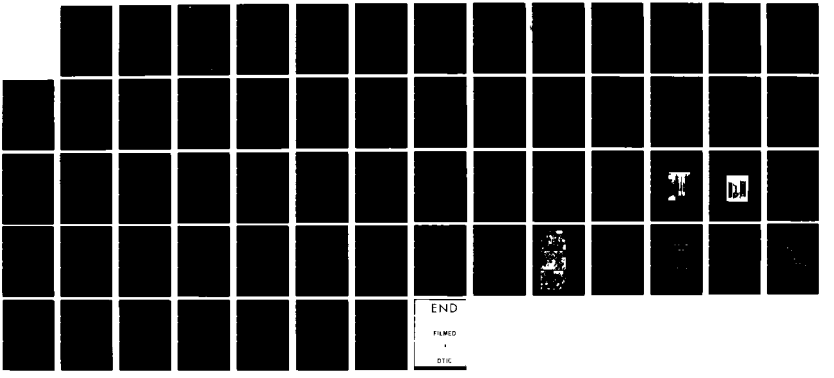

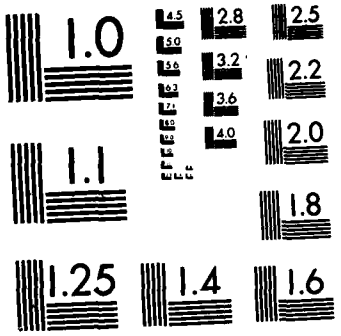

Final Technical Report

on

THE EFFECTS OF SMALL DEFORMATION ON CREEP AND STRESS RUPTURE BEHAVIOR OF ODS SUPERALLOYS

to

AFOSR/NE
Building 410
Bolling Air Force Base
Washington, DC 20332
Attn: Dr. A.H. Rosenstein

Vincent C. Nardone, Daniel E. Matejczyk and John K. Tien

Principal Investigator: Professor John K. Tien
Columbia University

Grant: AFOSR-78-3637

Report Date: 7 January 1983

Report Period: 1 June 1978 to 30 September 1982

UNCLASSIFIED

SECURITY CLASSIFICATION OF THIS PAGE (When Data Entered)

REPORT DOCUMENTATION PAGE		READ INSTRUCTIONS BEFORE COMPLETING FORM
1. REPORT NUMBER AFOSR-TR- 83-0095	2. GOVT ACCESSION NO. A125640	3. RECIPIENT'S CATALOG NUMBER
4. TITLE (and Subtitle) THE EFFECTS OF SMALL DEFORMATION ON CREEP AND STRESS RUPTURE OF ODS SUPERALLOYS		5. TYPE OF REPORT & PERIOD COVERED Final Technical Report 1 June 1978 to 30 Sept 1982
		6. PERFORMING ORG. REPORT NUMBER
7. AUTHOR(s) Vincent C. Nardone, Daniel E. Matejczyk and John K. Tien		8. CONTRACT OR GRANT NUMBER(s) AFOSR-78-3637
9. PERFORMING ORGANIZATION NAME AND ADDRESS Henry Krumb School of Mines Columbia University New York, NY 10027		10. PROGRAM ELEMENT, PROJECT, TASK AREA & WORK UNIT NUMBERS 61102F 2306/A1
11. CONTROLLING OFFICE NAME AND ADDRESS AFOSR/NE, Bldg. 410 Bolling Air Force Base Washington, DC 20332		12. REPORT DATE 7 January 1983
		13. NUMBER OF PAGES 57
14. MONITORING AGENCY NAME & ADDRESS(if different from Controlling Office)		15. SECURITY CLASS. (of this report) UNCLASSIFIED
		15a. DECLASSIFICATION/DOWNGRADING SCHEDULE
16. DISTRIBUTION STATEMENT (of this Report)		

Approved for public release;
distribution unlimited.

17. DISTRIBUTION STATEMENT (of the abstract entered in Block 20, if different from Report)

18. SUPPLEMENTARY NOTES

19. KEY WORDS (Continue on reverse side if necessary and identify by block number)

creep, stress rupture, cyclic creep, cyclic stress rupture, oxide dispersion strengthening, mechanical alloy, nickel-base alloy, notch strengthening

20. ABSTRACT (Continue on reverse side if necessary and identify by block number)

This Air Force sponsored research program studied the effects of predeformation including periodic load cycling on the creep and stress rupture of oxide dispersion strengthened (ODS) high temperature alloys. The alloys most studied in this program are Inconel MA 754, a Ni-Cr alloy strengthened by oxide dispersoids, and MA 6000, strengthened by both the oxide dispersoids and gamma prime precipitates. At temperatures above 1093°C, these alloys have better creep resistance than any current high temperature alloy. The MA 754 alloy is now used as stator

DD FORM 1 JAN 73 1473

UNCLASSIFIED

SECURITY CLASSIFICATION OF THIS PAGE (When Data Entered)

components in the hot sections of jet engines and MA 6000 is the only candidate turbine blade ODS alloy.

In contrast to behavioral trends in many other engineering materials, some enhancement of the creep and stress rupture resistance of the ODS alloys results from small amounts of deformation. First, hot isostatic pressing (HIP) treatments resulted in modest improvement in the creep resistance of MA 754 at 760°C. Second, notched specimens of MA 754 and MA 6000 showed an increase in the rupture life for a range of stresses at 760°C relative to smooth specimens at the same nominal stress. Greater than an order of magnitude increase in the rupture life was observed for some stress levels. Finally, small creep strains at a high stress result in creep property improvements at a lower stress at 760°C.

The main segment of the program focused on cyclic creep experiments, which involve repeated load changes having a period of a few minutes up to many hours, with tests being conducted on both MA 754 and MA 6000 . Cycling the load at 760°C resulted in a dramatic decrease in the minimum strain rate and an increase in the rupture life relative to static loading. The magnitude of the effect was shown to increase as the cyclic period decreased. In the case of a cyclic test on MA 6000 with a period of 10 minutes, an order of magnitude decrease in the minimum strain rate was observed. Such a large cyclic creep deceleration has been observed only for ODS alloys. The cyclic creep behavior of the ODS alloys is explained in terms of their ability to store and recover anelastic strain. The anelastic strain is shown to be responsible for the cyclic deceleration of ODS alloys.

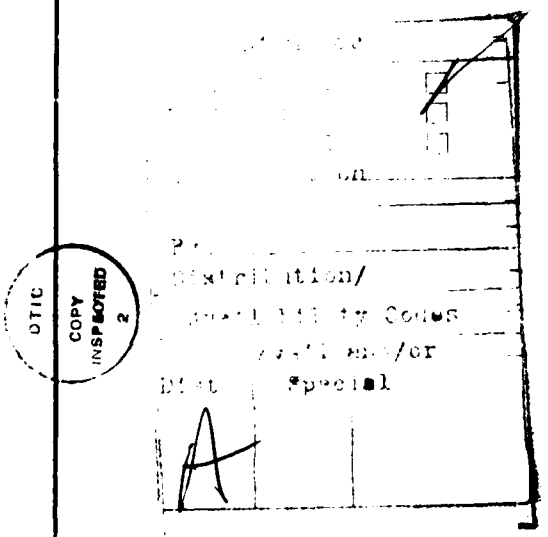

TABLE OF CONTENTS

ABSTRACT

This Air Force sponsored research program studied the effects of predeformation including periodic load cycling on the creep and stress rupture of oxide dispersion strengthened (ODS) high temperature alloys. The alloys most studied in this program are Inconel MA 754, a Ni-Cr alloy strengthened by oxide dispersoids, and MA 6000, strengthened by both the oxide dispersoids and gamma prime precipitates. At temperatures above 1093°C, these alloys have better creep resistance than any current high temperature alloy. The MA 754 alloy is now used as stator components in the hot sections of jet engines and MA 6000 is the only candidate turbine blade ODS alloy.

In contrast to behavioral trends in many other engineering materials, some enhancement of the creep and stress rupture resistance of the ODS alloys results from small amounts of deformation. First, hot isostatic pressing (HIP) treatments resulted in modest improvement in the creep resistance of MA 754 at 760°C. Second, notched specimens of MA 754 and MA 6000 showed an increase in the rupture life for a range of stresses at 760°C relative to smooth specimens at the same nominal stress. Greater than an order of magnitude increase in the rupture life was observed for some stress levels. Finally, small creep strains at a high stress result in creep property improvements at a lower stress at 760°C.

The main segment of the program focused on cyclic creep experiments, which involve repeated load changes having a period of a few minutes up to many hours, with tests being conducted on both MA 754 and MA 6000 . Cycling the load at 760°C resulted in a dramatic decrease in the minimum strain rate

and an increase in the rupture life relative to static loading. The magnitude of the effect was shown to increase as the cyclic period decreased. In the case of a cyclic test on MA 6000 with a period of 10 minutes, an order of magnitude decrease in the minimum strain rate was observed. Such a large cyclic creep deceleration has been observed only for ODS alloys. The cyclic creep behavior of the ODS alloys is explained in terms of their ability to store and recover anelastic strain. The anelastic strain is shown to be responsible for the cyclic creep deceleration of ODS alloys.

SUMMARY OF SIGNIFICANT FINDINGS

Studies have been carried out to determine the effect of small deformations in the form of (I) hot isostatic pressing (HIP), (II) small amounts of relatively high stress tensile creep deformation, and (III) the introduction of notches on the creep and stress rupture properties of ODS alloys. In addition, a large segment of the program was devoted to the study of the (IV) cyclic creep (repeated small deformations) behavior of the ODS alloys. The effect of the aforementioned deformations on the creep and stress rupture properties of the ODS alloys tested in air is given below.

I. Effects of Hot Isostatic Pressing

1. A modest improvement in the creep properties of MA 754 was found to occur when the material was given a HIP treatment at 1177°C.
2. There was no improvement in the creep properties of MA 754 when HIP treatments were performed at 1093°C and 1204°C.

II. Effect of High Stress Predeformation

1. The minimum creep rate of MA 754 was found to decrease as the amount of prestrain increased and was a factor of two lower at

1.2 percent prestrain at 760°C. The decrease in the creep rate is explained by the increase in the dislocation density, which occurs during the predeformation.

2. The predeformation did not adversely affect the rupture life and ductility of MA 754.

III. Effect of Notches

1. Notched specimens of MA 754 showed an increase in the rupture life for a range of stresses at 760°C relative to smooth specimens of the same diameter as the notched specimens at the root tip. The notch strengthening was observed for elastic stress concentrations of 3 and 10, the effect being greater for higher stresses.

2. Notched specimens of MA 6000 had rupture lives which were generally an order of magnitude greater than those of smooth specimens at 760°C. There was no significant difference between the notched and smooth specimens at 1093°C.

IV. Cyclic Creep Behavior

1. As the frequency of the load application increased, a dramatic decrease in the minimum strain rate and increase of the rupture life relative to static loading was observed for both MA 754 and MA 6000 . Cyclic creep deceleration of this magnitude has been observed only for ODS alloys.

2. The reason for the frequency dependent cyclic creep deceleration was shown to be the storage of anelastic strain during on load periods and its subsequent recovery during off load periods.

DETAILS OF THE EXPERIMENTAL RESULTS

Introduction

This program was aimed at documenting and understanding the effects of predeformation including periodic unloading on the creep and stress rupture of oxide dispersion strengthened (ODS) alloys. In particular, the two alloys most studied were Inconel MA 754 and Inconel MA 6000 . Inconel MA 754 is a Ni-Cr alloy containing Y_2O_3 dispersoids, while Inconel MA 6000 is strengthened by both the Y_2O_3 dispersoids and gamma prime precipitates. The principal areas of study included the effect of HIP treatments, high stress predeformation notches, and periodic unloading on the minimum strain rate and rupture life relative to what is observed for a static creep test on as received material.

Effects of Hot Isostatic Pressing (1)

The process of stress rupture in MA 754, as in many other particle strengthened systems, initiates under creep loading as a process of formation and coalescence of voids at transverse grain boundaries and inclusions due to high localized triaxial stresses at grain boundaries and at particle matrix interfaces (2-5). The decohesion at these highly stressed regions results in the development of cracks and loss of load bearing area, which in turn can rapidly load to failure. However, a small amount of deformation that did not itself open up cracks might effectively inhibit the decohesion that marks the onset of the stress rupture process. The compressive nature of a HIP treatment allows predeformation to occur without the problems of tensile precracking.

Three HIP treatments were applied to MA 754 as follows: 1093°C/138 MPa/2 hours; 1177°C/138 MPa/2 hours; 1204°C/138 MPa/2 hours. The HIP conditions were chosen to bracket the usual HIP conditions as applied to superalloys.

Creep testing was carried out at 760°C and 1093°C on the HIP-1093°C and HIP-1204°C specimens under constant tensile load. Due to a lack of material, testing on the HIP-1177°C specimens was done only at 760°C.

The HIP-1093°C and HIP-1204°C treatments resulted in no detectable improvement in the creep properties of MA 754 at 760°C and 1093°C. Neither the rupture life nor the minimum strain rate changed significantly relative to tests performed on virgin material. Some representative results are given in Figures 1 and 2 for the HIP-1204°C treatment for tests conducted at 760°C.

For the HIP-1177°C treatment, however, positive effects were observed for tests performed at 760°C. The minimum creep rates were decreased relative to the standard material as shown in Figure 3, while the rupture lives were improved by a factor of approximately 1.5 over the range of applied stresses as given in Table I. Inspection of the HIP-1177°C creep curves revealed that the HIP treatment apparently caused a delay in the time to the onset of tertiary creep by about 50 percent as compared to the standard material. A representative comparison of the creep curves is shown in Figure 4. The final ductilities were unaffected by the HIP treatment, but the time spans in tertiary were increased by 30 to 80 percent; see Figure 4 and Table I.

It is conceivable that the HIP-1177°C treatment may be suppressing crack initiation, and thus tertiary creep, by delaying the separation of the particles from the matrix. Two possible explanations for an improved particle-matrix bonding are a pressure assisted diffusion bonding process or a residual stress relief at the particle-matrix interface during the HIP process.

Effect of High Stress Predeformation (6)

The effect of predeformation at either ambient or elevated temperature on the creep and stress rupture behavior is of engineering importance since predeformation may either improve or deteriorate subsequent mechanical behavior of heat resistant alloys. It has recently been shown that large deformation of γ' strengthened superalloy causes void formation at grain boundaries and results in a degradation of creep and stress rupture properties (7,8). For a smaller amount of deformation for which voids are not formed, the results show in some cases improvement of the mechanical properties (9), while in another study degradation in properties was reported (10). In view of these results for the γ' strengthened superalloys, it would be interesting to investigate the effect of predeformation on an oxide dispersion strengthened heat resistant alloy.

The specimens of MA 754 were predeformed by applying an initial stress of 276 MPa at 760°C until a desired amount of strain was attained. Prestrain values of 0.3 percent, 0.6 percent, 0.9 percent, and 1.2 percent were chosen in order to fall within the primary region of the creep curve at 276 MPa and 760°C. The load was then reduced to give a stress of 224 MPa, and the specimens were then crept to failure at the same temperature of 760°C.

Optical and scanning microscopic observations of specimens after prestraining revealed no obvious grain structure changes, void formation, or cracking at grain boundaries. However, TEM studies showed that the average dislocation density increased with increasing prestrain as shown in Figure 5.

A plot of the strain rate versus time is shown in Figure 6 for the standard (no prestrain), 0.6 percent and 1.2 percent prestrained specimens. It

is found that the time to reach the minimum creep rate decreases as the amount of prestrain increases, that is, durations of primary creep appear to be shortened with predeformation. A plot of minimum creep rates at 224 MPa versus amount of prestrain at 274 MPa represented in Figure 7 indicates that the minimum creep rates decrease with increasing amounts of prestrain. Note that the minimum strain rate is decreased by a factor of two for the 1.2 percent prestrain relative to the standard. The rupture life and the creep ductility were not adversely affected by the prestrain.

The decrease in the minimum strain rate and the shortened durati of primary creep are consistent with the observed dislocation density in ıse due to the predeformation. The creep strength of particle strengthen ' _loys is directly related to the flow stress at the creep temperature and the creep strain rate (11). The matrix flow stress (σ) on the other hand can vary with the dislocation density (ρ) as $\sigma = \alpha\mu b\sqrt{\rho}$ (12), where α is a factor about equal to 0.5, μ is the shear modulus, and b the Burgers vector. We therefore propose that the creep strengthening effects observed are due to work hardening effects resulting from dislocation-dislocation interactions, which in turn increase the flow stress of the material.

Effect of Notches (13)

This segment of the program documented the effect of notches on the rupture life of the ODS alloys MA 754 and MA 6000 . Two different specimen designs were used which resulted in calculated elastic stress concentration factors, K_t, of 3 and 10. Round specimens (see Figure 8) circumferentially notched had a calculated K_t value of 3, while flat specimens (see Figure 9) notched on opposite sides of the gage section had a K_t value of 10. The design of the smooth bar and the circumferentially notched specimens were such that the gage diameter of the smooth specimens was equal to the diameter

of the notched specimens at the root of the notch. Such a design allows comparison of stress rupture results from smooth bar and notched bar specimens without the need to consider possible gage diameter results. The flat specimens were designed so that the cross sectional area between the two notches was the same as the cross sectional area in the gage section of a smooth bar specimen.

The results from the stress rupture tests at 760°C for MA 754 are shown in Figure 10. The stress rupture life is always greater for notched specimens than for unnotched specimens, and the amount of improvement increases with stress. At 207 MPa and 760°C, the ratio of the notched (K_t = 3) to unnotched rupture life is about 1.5. At 241 MPa and 760°C, this ratio has increased to 16.5.

The results from the stress rupture tests at 760°C for MA 6000 are shown in Figure 11. Once again, significant notched strengthening is observed. In this case, however, the strengthening effect appears to be independent of the applied stress. The rupture life of the notched specimens (K_t = 3) is approximately an order of magnitude greater than that of smooth specimens.

Last, the stress rupture results for MA 6000 at 1093°C are shown in Figure 12. The introduction of the notch (K_t = 3) does not appear to have any significant effect on the rupture life.

The results presented above are somewhat surprising in light of general observation that notch weakening is observed when the ductility of a material is $\leq$5 percent (14-17). Both MA 6000 and MA 754 have limited creep ductility. The observed strengthening may arise from a deformation hardening effect. In the previously mentioned study of the effect of predeformation on the creep

properties of MA 754, it was shown that predeformation which does not open cracks can result in a reduction of the creep rate. Stress relaxation at the notch root could have a similar strengthening effect.

It should also be noted that the strengthening effect is greater for $K_t = 3$ than it is for $K_t = 10$ (see Figure 8). Perhaps the relaxation effect at the notch tip is optimal for $K_t = 3$. The relaxation in the case of the very sharp cracks ($K_t = 10$) might lead to cracking. Thus, greater strengthening would be observed for $K_t = 3$ relative to $K_t = 10$.

An alternative explanation for the longer stress rupture lives of notched specimens of MA 754 and MA 6000 may be that the notch constrains the creep fracture path to a limited volume of material. Thus, crack growth is constrained to a path markedly different from the normal fracture path in uniaxial stress rupture. For MA 754, the stress rupture at 760°C is intergranular with decohesion of transverse grain boundaries. Eventually the fracture path links up these transverse boundaries. For MA 6000 stress rupture at 760°C, the fracture is transgranular along planes of maximum shear stress at roughly 45° to the specimen axis. In both cases, the "notch strengthening" effect may be simply the effect of the specific stress distribution in the notched bar (a localized triaxial stress rather than a uniform uniaxial stress), and the notch effect is the effect of this nonhomogeneous stress distribution on the crack growth process.

Cyclic Creep Behavior (18,19)

Many alloy applications that involve stress and high temperature use static creep data for design criteria. In most real situations, however, a machine rarely experiences a static load during its entire life. Rather, the load is normally applied in a cyclic manner. A pertinent example of cyclic load application during the service life of ODS alloys would be the running and subsequent shutdown of a jet engine. In addition, simply varying the thrust of a jet engine while it is already running corresponds to cyclic load application. It was with this in mind that we began studying cyclic creep of ODS alloys. The basic question of practical interest we sought to answer was the effect that load cycling had on the minimum strain rate and the rupture life. Thus, this will allow one to determine how conservative are the current design criteria. Also, the explanation of any observed effects is of great scientific interest.

Experimental Arrangement:

The cyclic creep experiments require a capability to apply loads like that shown schematically in Figure 13. The load and time parameters must be controllable over a wide range. The load transient must have no overshoot due to inertial effects or shock loading effects. During this project year, we modified several Satec high temperature static creep test machines to obtain the required loading control. Figure 14 is a schematic representation of our cyclic creep test system. The system retains features of the Satec machine such as load train universal joints and automatic specimen realignment to minimize bending moments in the specimen. Displacement is monitored using an Applied Test Systems high temperature extensometer connected to a Hewlett Packard displacement transducer. Displacement signals were recorded on paper chart recorders or by using a Digital Equipment

Corporation MINC data acquisition system, which was installed for strain recording and analysis.

The cyclic loading system is a simple and inexpensive addition to the static creep lab equipment. It is a device that changes the creep machine pan load in a very controlled manner. As shown in the schematic (Figure 14), an electronic timer controlled lifting mechanism changes the load. The damped spring arrangement is a very important component of the load change system. If an incremental load is suddenly applied to the creep machine pan, the specimen experiences a load overshoot due to the inertia of the system. Design of the carrying spring and selection of the load change rate assure that the load inertial overshoot will be infinitesimal.

The creep machine load change equipment includes a microcomputer time controller, a surplus aircraft actuator, and various hand-made parts. It is a very inexpensive design (total cost approximately $300), and it gives us the required precise, controllable load changes.

For the first few cyclic creep experiments, the displacement signals were recorded solely on paper chart recorders. Subsequently, however, a MINC computer was interfaced with the data acquisition system. The MINC is capable of giving a continuous plot of strain as well as strain rate versus time while the test is still in progress. This continuous feedback of results allows one to switch between cyclic and static testing at specific intervals during a single test. As will be seen, this type of testing was necessary to explain the reason for the cyclic creep behavior of the ODS alloys.

The MINC also provides the capability to analyze the cyclic data on a

fine scale, cycle-by-cycle basis. The enhanced resolution of the displacement signals, which is given by the MINC, was used to confirm our explanation of the observed cyclic creep behavior.

A series of cyclic creep tests was performed on both MA 754 and MA 6000E. The load was cycled such that the time at maximum load equaled the time at minimum load. The minimum load (41 MPa) was slightly positive in order to maintain tension and alignment in the load train. The hold times (one-half the cyclic period) ranged from 10 hours to 5 minutes, which is equivalent to a square wave loading frequency of 0.05 hrs^{-1} to 6 hrs^{-1}. The load change was accomplished in approximately 15 seconds.

Experimental Results:

Figure 15 shows a typical creep curve for this type of cyclic creep experiment. This curve is for the 10-hour cyclic period (five hours on load, five hours off load) test for MA 754. During the off-load cycle, negative straining can be seen. This is an important feature in cyclic creep behavior as will become apparent. Figure 15 also shows the envelope strain. The envelope strain is plotted versus time on load to generate a cyclic creep curve and determine the minimum strain rate of the cyclic test.

Table II summarizes the principal experimental results for MA 754 for all frequencies and all applied stresses. Two separate sets of specimens, processed slightly differently, were used in the experiments, and thus the stress rupture data in Table I are separated according to specimen lot. The minimum creep rate results for the two sets of specimens were comparable and did not need to be considered separately.

Table III summarizes the principal experimental findings for Inconel

MA 6000 . The cyclic tests with periods of 40 minutes and 10 minutes were run for 200 hours on load (400 hours total time) before they were interrupted. Both specimens were creeping at reasonably constant creep rates when they were interrupted.

As is evident in Tables II and III, a dramatic decrease in the minimum strain rate and increase in the rupture were found to accompany an increase in the loading frequency for both MA 754 and MA 6000 . Such a dramatic deceleration of the creep rate during cyclic loading has been observed only for ODS alloys. Some representative cyclic creep curves and creep rate versus time plots are given in Figures 16 and 17. These graphs clearly illustrate the dramatic deceleration of the creep rate relative to static loading for both MA 754 (Figure 16) and MA 6000 (Figure 17).

It should be noted that the cyclic creep strengthening exhibited by these ODS alloys is in sharp contrast to what is observed for Udimet 700, a conventional superalloy. The rupture life of Udimet 700 actually decreases in the frequency range where a large increase in rupture life is seen for the ODS alloys. A comparison of the rupture life behavior as a function of frequency is shown in Figure 18 for MA 6000 and Udimet 700. The ODS alloy clearly possesses superior cyclic creep properties. Also, in the limit of very high frequencies, our results suggest that the rupture lives of ODS alloys may become infinite. However, high cycle fatigue tests on ODS alloys shows that failure does occur. These HCF tests indicate that the cyclic strengthening reported in this study could possibly reach a plateau or begin to reverse at very high frequencies.

Explanation of the Cyclic Creep Behavior:

The explanation for the reduction of the creep rate can be deduced by examining Figure 19. Figure 19 is a copy of typical data taken by a chart recorder connected to a LVDT during a cyclic creep test of MA 6000.. The cyclic period for the test was 40 minutes, a frequency at which the deceleration of the creep rate was substantial. There is a striking symmetry between the on-load and off-load portions of the figure. That is, the magnitude and time dependence of the strain being accumulated on load are similar to those being recovered off load. The recovery of strain during the off-load periods, i.e., anelastic strain, is responsible for the creep deceleration. Anelastic strain is defined here as time dependent recoverable strain.

The way in which the storage and recovery of anelastic strain can result in cyclic creep deceleration can be explained as follows. During the time at maximum load, the apparent creep strain is acutally composed of two parts: a nonrecoverable strain and an anelastic strain. The anelastic portion of the strain at maximum load does not contribute to the net creep rate, however, since it is capable of being recovered during the time at minimum load. The repeated storage and recovery of the anelastic strain during a cyclic creep test results in the creep deceleration.

A series of tests and experimental observations were made to confirm that the mechanism involving anelastic strain was responsible for the creep deceleration. A brief summary of these critical observations will be given first for MA 754 and then for MA 6000 .

TEM dislocation microstructures (see Figure 20) and SEM fractography of MA 754 indicate no loading mode or cyclic frequency dependent change in mode of deformation or mode of fracture. No TEM evidence was found to indicate a

microstructural hardening, which could account for a reduction in the cyclic creep rate.

Tests on MA 754 were run with loading mode changes from static to cyclic (cyclic period 10 minutes) or from cyclic to static. In all cases, within 10 minutes of the mode change the strain rate agreed with corresponding results for constant mode tests (those test results listed in Table II). The cyclic strain rate effect being immediate and reversible with loading mode changes is consistent with the anelastic mechanism. The cyclic frequency dependent creep rates cannot be attributed to cyclic work hardening of the material.

A mixed mode test was also performed for MA 6000 . In going from static to cyclic load application at a period of 40 minutes, the creep rate immediately decelerated. In fact, the net creep rate was negative during the initial portion of the cyclic load application as shown in Figure 21. The only reasonable explanation for this result is in terms of anelastic strain recovery. More anelastic strain was being recovered during the off-load periods than the total strain occurring during the on-load periods. This was possible due to the storage of anelastic strain which occurred during the static load application A positive creep rate did not resume until the specimen had been on load for ~20 hours.

To illustrate that the magnitude and time dependence of the total on-load strain relative to the anelastic strain was sufficient to cause deceleration of the creep rate, a point-by-point subtraction of strain accumulated on load less the strain recovered during the previous off-load period was made for MA 6000 . The pivoting assumption is that the anelastic strain recovered during an off-load period must be stored before nonrecoverable

creep will occur. The point-by-point subtraction was done via a MINC computer, which took a voltage reading every 5 seconds. The result for such a subtraction is shown in Figure 22 for a test run at a period of 2 hours. The upper curve is the on-load portion of a single cycle. The lower curve is a point-by-point subtraction of the upper curve less the anelastic strain recovered during the previous off-load period. Notice that strain is not accumulated until approximately 20 minutes have elapsed. Thus, it is evident that the magnitude and time dependence of the net creep strain (on-load strain minus anelastic strain) is capable of resulting in the deceleration of the creep rate.

The data given in Figure 22 are just one of many point-by-point subtractions performed on various cycles. Although the time at which the lower curves began to show strain being accumulated varied from one cycle to another, the shape of the curves was still the same. There was a period of zero or slightly negative net strain followed by strain being accumulated at approximately the same rate as the steady state creep rate of the upper curve. The data shown in Figure 22 were chosen as characteristic since the period of zero strain generally ranged from 10 to 30 minutes.

The aforementioned experimental tests and observations present overwhelming evidence that the cyclic creep deceleration is indeed the result of the storage and recovery of anelastic strain.

Development of a Phenomenological Model:

The physical nature of creep can lead to some simple assumptions, which enable derivation of a phenomenological equation for the observed frequency dependent creep rate reduction in the typical ODS alloy studied. As creep

proceeds in a strengthened microstructure, the motion of dislocations is impeded by dispersoids, by dislocation tangles, by grain boundaries, and by possibly other microstructural features (3). As a creep stress is first applied, the initial dislocation configuration change will be to move in a relatively unimpeded manner until the back stresses arising from the microstructural feature are developed. This initial configuration change might, for example, be the bowing of dislocations between the oxide dispersoids. The back stress developed can arise from the resulting bowed dislocation's line tension, long range dislocation network interactions, etc.

If the stress is removed while this configuration change is in progress, the strain may be recovered anelastically and almost completely while, if the stress is held at the initial level for longer periods, dislocation will escape the strengthening interactions, providing non-recoverable strain after an initial delay due to the anelastic strain storage period. This point of view is depicted in Figure 23, where the total on-load strain is the sum of the non-recoverable creep strain, ε_{cr}, and the anelastic strain, ε_{an}, which is the time-dependent, recoverable strain.

Accordingly, we are proposing that the storage of anelastic strain immediately following load application and its recovery following load removal can offset the delayed non-recoverable creep, and thus cause cyclic creep deceleration. At high loading frequencies, more of the on-load strain is recoverable than at low frequencies. With the above physical model and some simplifying assumptions about the form of the creep delay, the frequency dependent cyclic strain rate function can be derived.

First, it is assumed that the anelastic strain saturates as an exponential function

$$\varepsilon_{an}(t) = \varepsilon_{an\ total}(1-\exp(-(t/t^*))) \qquad (1)$$

where ε_{an} is the anelastic strain as a function of time after loading, $\varepsilon_{an\ total}$ is the total anelastic strain stored at the given stress level, and t* is a characteristic time. This exponential decay functional dependence is very close to our observed anelastic relaxation, typically shown in Figure 23. This dependence is also observed in several other studies dedicated to the anelastic strain relaxation phenomenon (22,23).

Following the load transient, the rate of non-recoverable creep, $\dot{\varepsilon}_{cr}$, eventually reaches the static creep rate as Figure 23 illustrates. We next assume that this non-recoverable creep rate is proportional to the amount of anelastic strain stored up to that time, and therefore, following Equation (1), the rate of non-recoverable creep at any instant following the load application is

$$\dot{\varepsilon}_{cr}(t) = \dot{\varepsilon}_{sc}(1-\exp(-(t/t^*))). \qquad (2)$$

To obtain the frequency dependent evvelope minimum strain rate, this instantaneous creep rate can be averaged over the on-load period ($\Delta t = 1/2\nu$, $\nu \equiv$ the cyclic frequency of the square wave)

$$\dot{\varepsilon}^{\text{envelope}}_{\text{cyclic}}(\nu) = \frac{\int_0^{\Delta t} \dot{\varepsilon}_{cr}(t)dt}{\Delta t} = \dot{\varepsilon}_{sc}(1+2\nu t^*(\exp(-1/2\nu t^*)-1)) \qquad (3)$$

Figure 24 shows that this function and the cyclic creep data agree reasonably well when the static creep rate is that from the static creep experimental data (for the 221 MPa maximum stress case for MA 754), and t* is adjusted to obtain the least squares fit to the data. Insufficient per cycle

data preclude the quantitative fitting of Equation (3) to the envelope creep rates obtained at the two other maximum applied stress levels for MA 754. The best fit t* is 0.48 hours for MA 754 and 2.5 hours for MA 6000 . This is somewhat off the time constant directly measured from an experimental anelastic relaxation, where t* was measured to be 0.2 hours for MA 754 and 0.25 hours for MA 6000..

The above exercise is useful, however, because it shows that this approach can model the data reasonably well, and the t* obtained from curve fitting is the same order of magnitude as the experimental relaxation time constant.

The creep rate ratio might also be termed, in this case, the creep/fatigue interaction parameter. This is the factor by which the cyclic creep is decelerated relative to static creep, where

$$\frac{\dot{\varepsilon}_{\text{envelope}}(\nu)}{\dot{\varepsilon}_{sc}} = 1+2\nu t^*(\exp(-1/2\nu t^*)-1) \qquad (4)$$

Accordingly, the anelastic relaxation time constant, t*, is the parameter which is especially relevant to understanding of the role of back stress in cyclic creep. Complete understanding would require understanding of the anelastic mechanism, the back stress magnitude as a function of anelastic strain, and the kinetics of the relaxation.

CONCLUDING REMARKS

Studying the effect of HIP treatments on the minimum strain rate and rupture life of ODS alloys represents an effort to improve the creep properties of these alloys. The program has shown what HIP conditions result in an improvement of the creep properties. Just as important, however, the HIP conditions that do not improve creep properties were also documented. Thus, the range of conditions where one can and cannot expect a modest improvement in the creep properties of ODS alloys as a result of HIP treatments has been established.

High stress predeformation simulates the load overshoots which inevitably occur during the operation of a jet engine. This scientific study has shown that high stress predeformation does not degrade the creep properties of MA 754, but actually results in a decrease in the minimum strain rate relative to a standard static creep test. The important qualification of these beneficial effects is that the predeformation be small enough so that no cracks are initiated. The decrease in the minimum strain rate was shown to result from an increase in the dislocation density during the predeformation. Thus, this part of the study has established under what conditions predeformation can improve the creep properties of MA 754 and why this improvement occurs.

Determining the effect of notches on the creep properties of ODS alloys is important since all engines contain notches. How a material will respond to the introduction of notches is therefore of practical significance. This systematic study has shown that ODS alloys are in fact capable of notch strengthening, although their stress rupture ductility is relatively small.

Perhaps the single most important result of this study is the documentation of the cyclic creep behavior of ODS alloys. This program has shown that ODS alloys are capable of dramatic cyclic creep deceleration as evidenced by a decrease in the minimum strain rate as much as an order of magnitude, and increase in the rupture life relative to static creep. Cyclic creep deceleration of this magnitude has not been seen before for any class of alloys. The basic understanding resulting from this program shows that the cyclic creep deceleration is due to the storage and recovery of anelastic strain. The results are especially important because the cyclic creep effects occur for the temperature, stress, and frequency of loading generally experienced by some components of a jet engine.

REFERENCES

1. A. Koren: Master's Thesis, Columbia University, 1979.
2. T.E. Howson, D.A. Mervyn and J.K. Tien: Met. Trans. A, 1980, Vol. 11A, p. 1690.
3. T.E. Howson, J.E. Stulga and J.K. Tien: Met. Trans. A, 1980, Vol. 11A, p. 1599.
4. A.S. Argon and J. Im: Met. Trans. A, 1975, Vol. 6A, p. 839.
5. D.H. Killpatrick, A. Phillips and V. Kerlins: Trans. AIME, 1968, Vol. 242, p. 1657.
6. R.T. Marlin, F. Cosandey and J.K. Tien: Met. Trans. A, 1980, Vol. 11A, p. 1771.
7. B.F. Dyson and D.E. Henn: J. Microsc., 1973, Vol. 97, p. 165.
8. B.F. Dyson, M.S. Loveday and M.J. Rogers: Proc. R. Soc. London, 1976, Vol. 349, p. 245.
9. J.M. Oblak and W.A. Owczarski: Met. Trans., 1972, Vol. 3, p. 617.
10. W.C. Harrigan, Jr., C.R. Barrett and W.D. Nix: Met. Trans., 1974, Vol. 5, p. 205.
11. J.H. Hausselt and W.D. Nix: Acta Metall., 1977, Vol. 25, p. 595.
12. S. Takeuchi and A.S. Argon: J. Mat. Sci., 1976, Vol. 11, p. 1542.
13. F. Nami: Master's Thesis, Columbia University, 1979.
14. "Metals Handbood," eighth edition, Vol. 1, pp. 473-476, ASM, Metals Park, Ohio, 1961.
15. "Metals Handbook," eighth edition, Vol. 8, pp. 249-252, ASM, Metals Park, Ohio, 1975.
16. P. Shahinian, Trans. ASME, 1965, p. 344.
17. T.K. Glasgow and M. Quativetz, NASA TM X-3303, Washington, D.C., October 1975.

18. D.E. Matejczyk, Y. Zhuang and J.K. Tien: Met. Trans. A, in press.

19. V.C. Nardone: Master's Thesis, Columbia University, 1982.

20. C.T. Yen: Master's Thesis, Columbia University, 1981.

21. R.T. Marlin and J.K. Tien: unpublished research, Columbia University, 1981.

22. J.D. Lubhan: Trans. ASM, 1953, Vol. 45, p. 787.

23. W.J. Evans and G.F. Harrison: Scripta Met., 1975, Vol. 9, p. 239.

LIST OF FIGURES

Fig. 14. Schematic diagram of the cyclic creep testing system.

Fig. 15. Strain versus time for an entire cyclic creep test of MA 754; cyclic frequency 0.1 hr^{-1}, load 221.41 MPa.

Fig. 16. (a-c) Envelope strain versus time on load for the range of cyclic loads and cyclic frequencies for MA 754; (d-f) Envelope strain rate versus time on load for the same tests.

Fig. 17. (a) A static and three cyclic creep curves for MA 6000 with hold times of 3 hours, 1 hour, and 5 minutes. (b) A differential plot of 5(a) represented as the log of the strain rate versus time on load.

Fig. 18. Rupture life versus cyclic frequency for MA 6000 and Udimet 700, a conventional superalloy.

Fig. 19. Copy of typical data for MA 6000E taken by a chart recorder connected to a LVDT for a test with a period of 40 minutes.

Fig. 20. TEM dislocation microstructures for test specimens of MA 754 interrupted at 1.5 percent strain for (a) 221 MPa static load, (b) 221.41 MPa cyclic load at 0.5 cycles/hour, and (c) 221.41 MPa cyclic load at 6 cycles/hour.

Fig. 21. Strain versus time on load for the mixed mode test of MA 6000 ; the marks indicate when the change in the mode of load application occurred.

Fig. 22. The upper curve is the total strain on load versus time. The lower curve is a point-by-point subtraction of the total strain on load (versus time) less the anelastic strain (versus time) of the previous cycle, defined here as net strain. These results are for the MA 6000 test with a period of two hours.

Fig. 23. Strain versus time for one cycle of the MA 754 cyclic creep test at 0.5 cycles per hour and 221.41 MPa.

Fig. 24. Ratio of the cyclic to static strain rate versus frequency for MA 754 and MA 6000 . The line is derived from Equation (3) with the best fit value being chosen for t*.

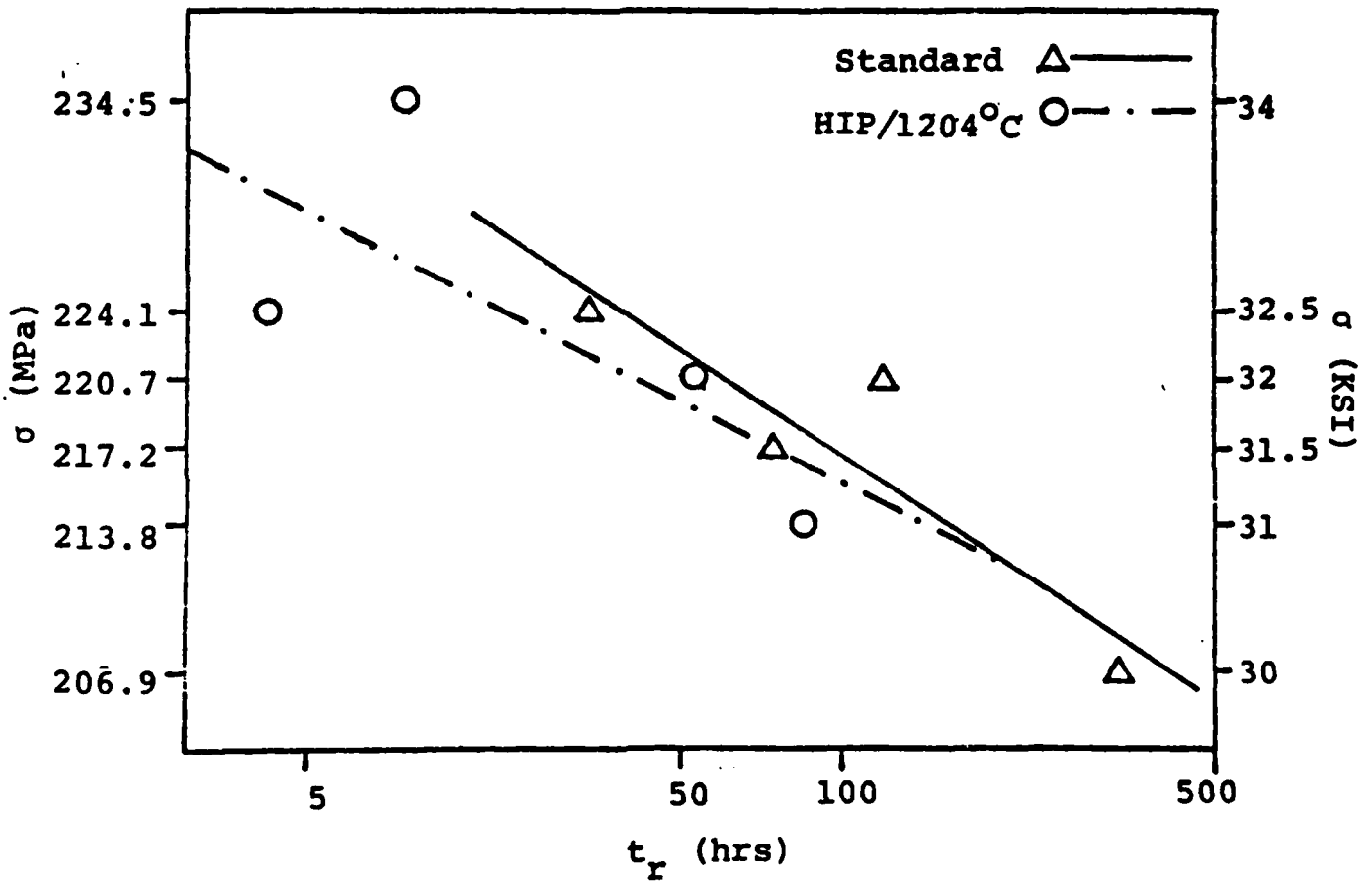

Fig. 1. Applied stress versus rupture life of MA 754 at 760°C for virgin material and for material after HIP treatment of 1204°C/138MPa/2 hrs.

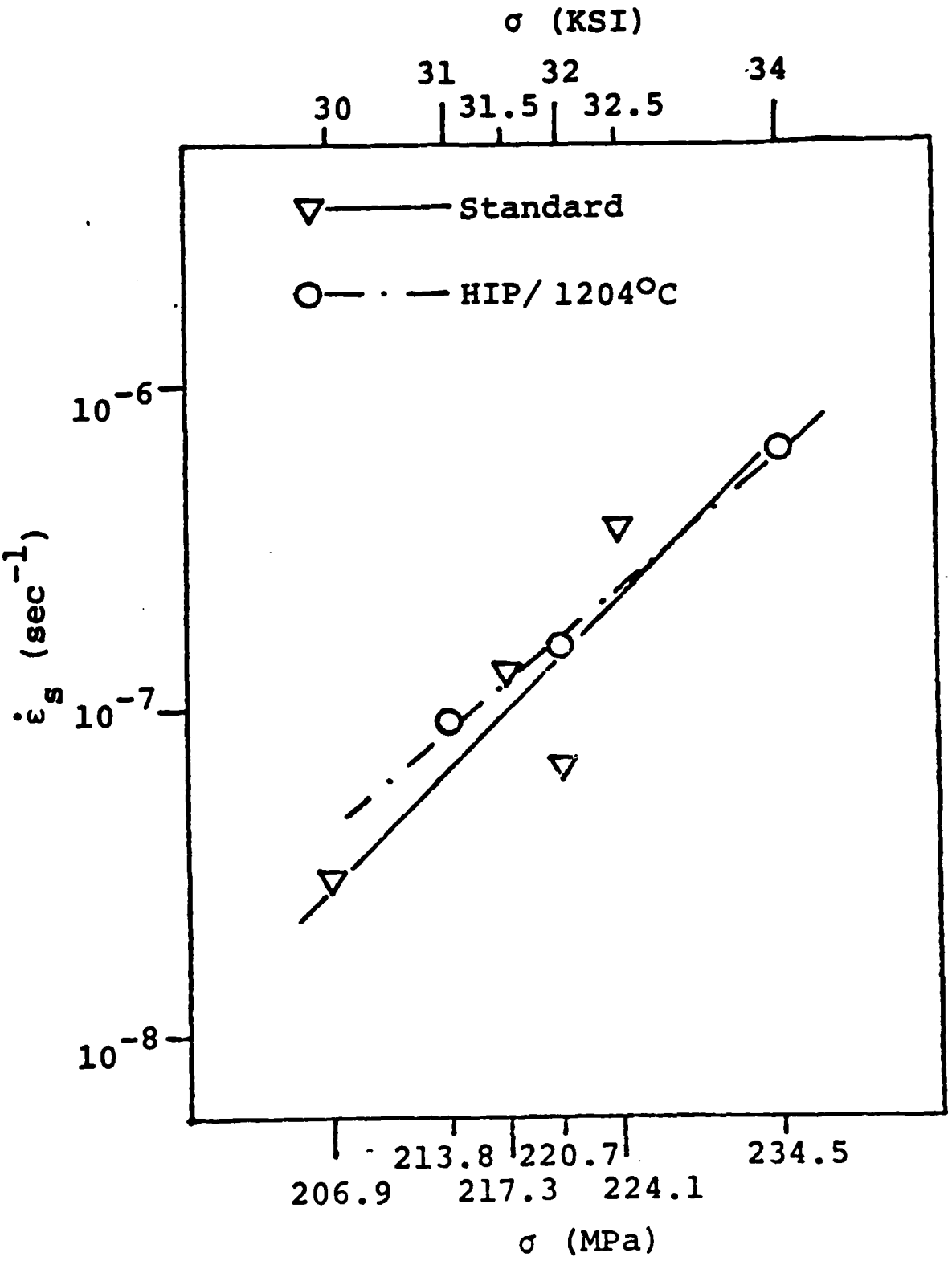

Fig. 2. Creep rate versus applied stress at 760°C for MA 754 virgin material and material after HIP treatment of 1204°C/138MPa/2 hrs.

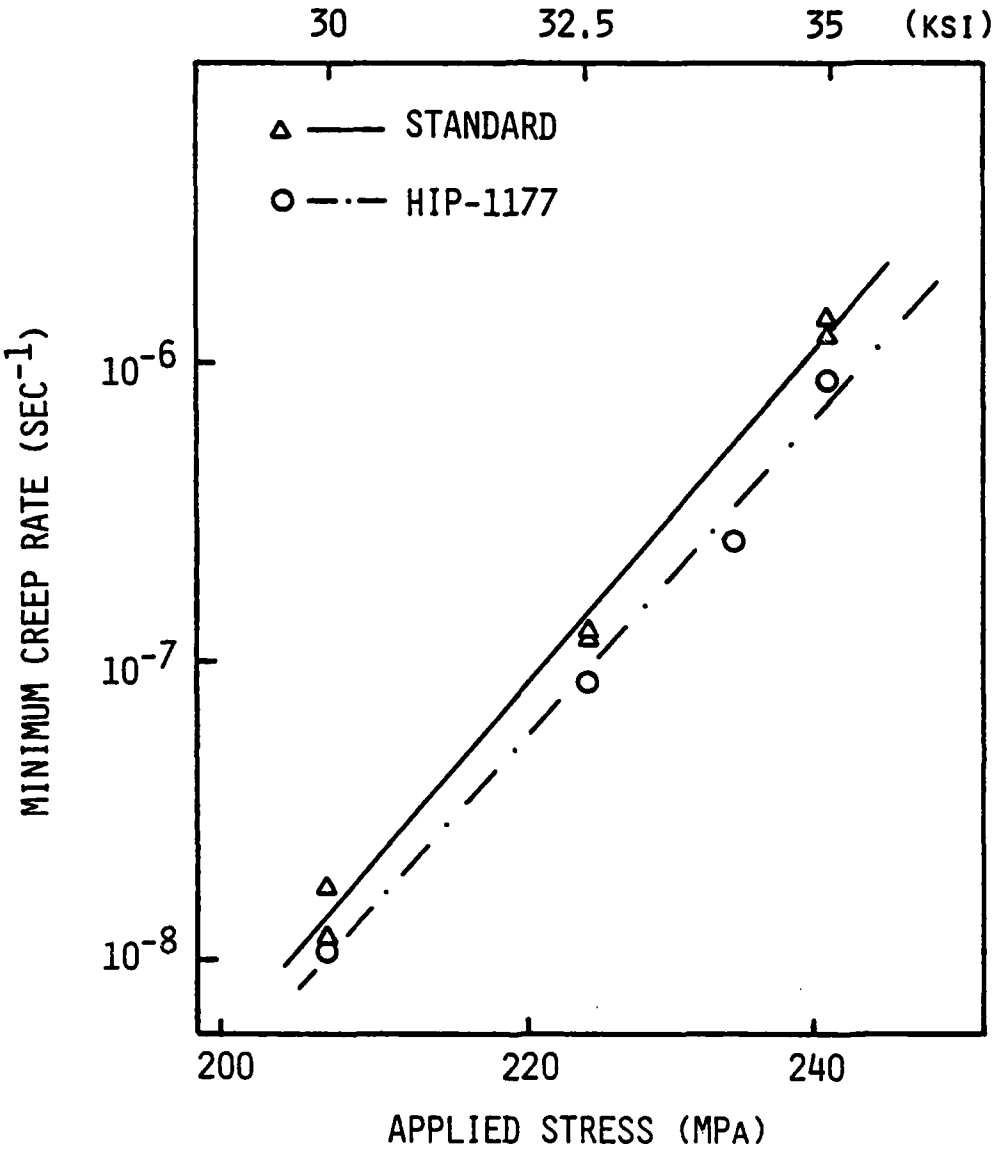

Fig. 3. Minimum creep rate versus applied stress at 760°C for standard MA 754 material and HIP-1177 material.

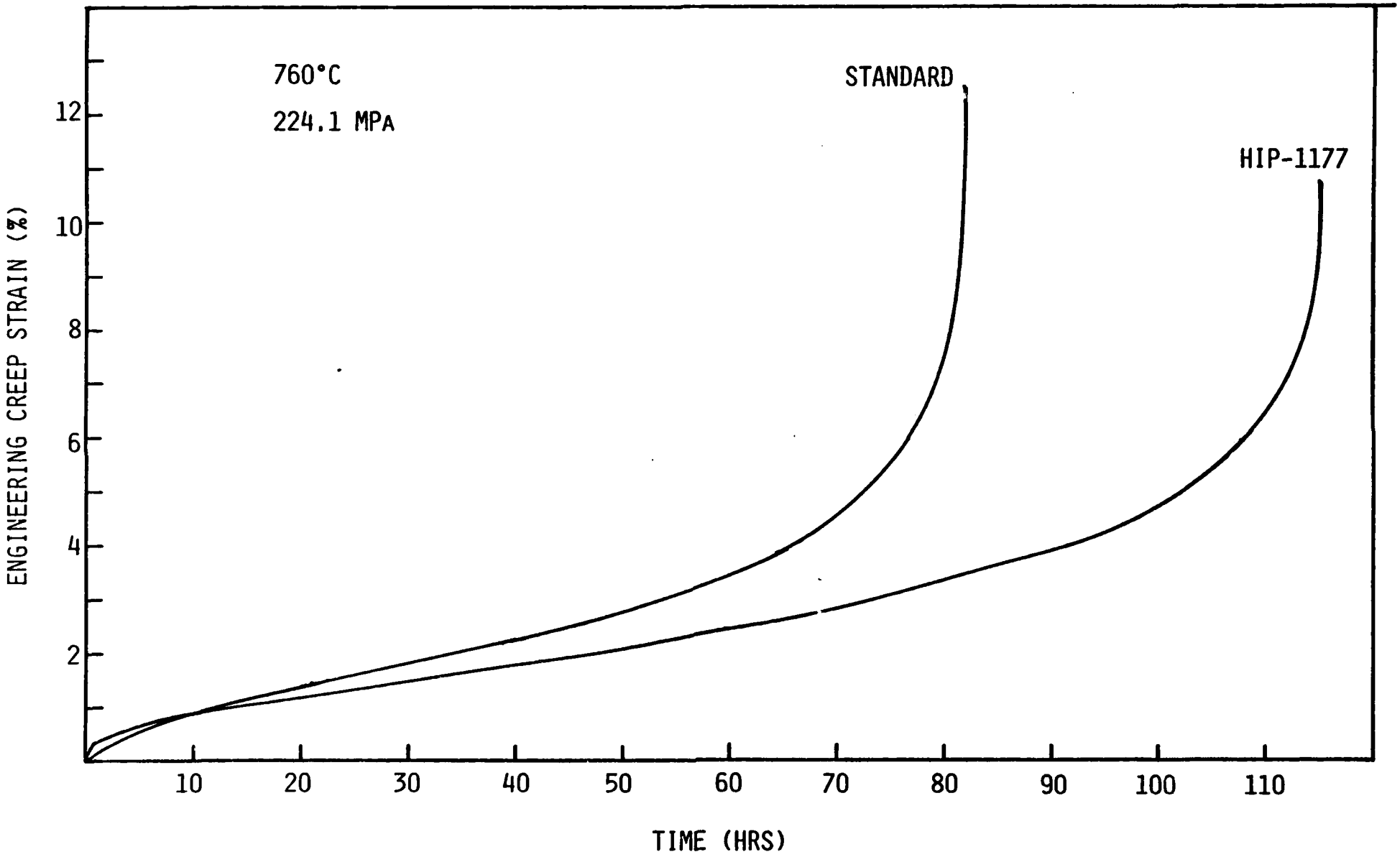

Fig. 4. Comparison of 760°C, 224.1 MPa creep curves for standard MA 754 material and HIP-1177 material.

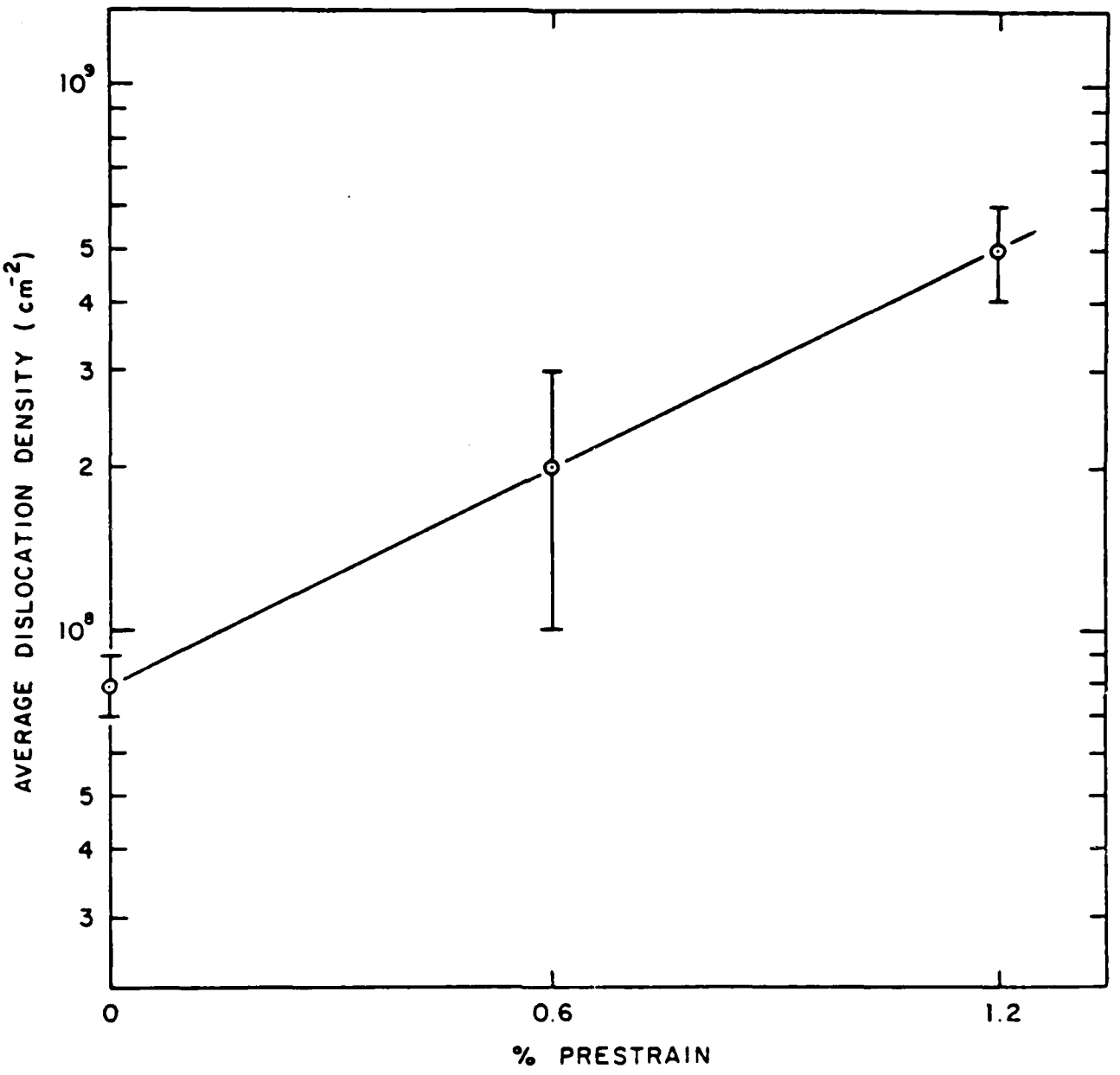

Fig. 5. Average dislocation density as a function of prestrain at 276 MPa and 760°C for MA 754.

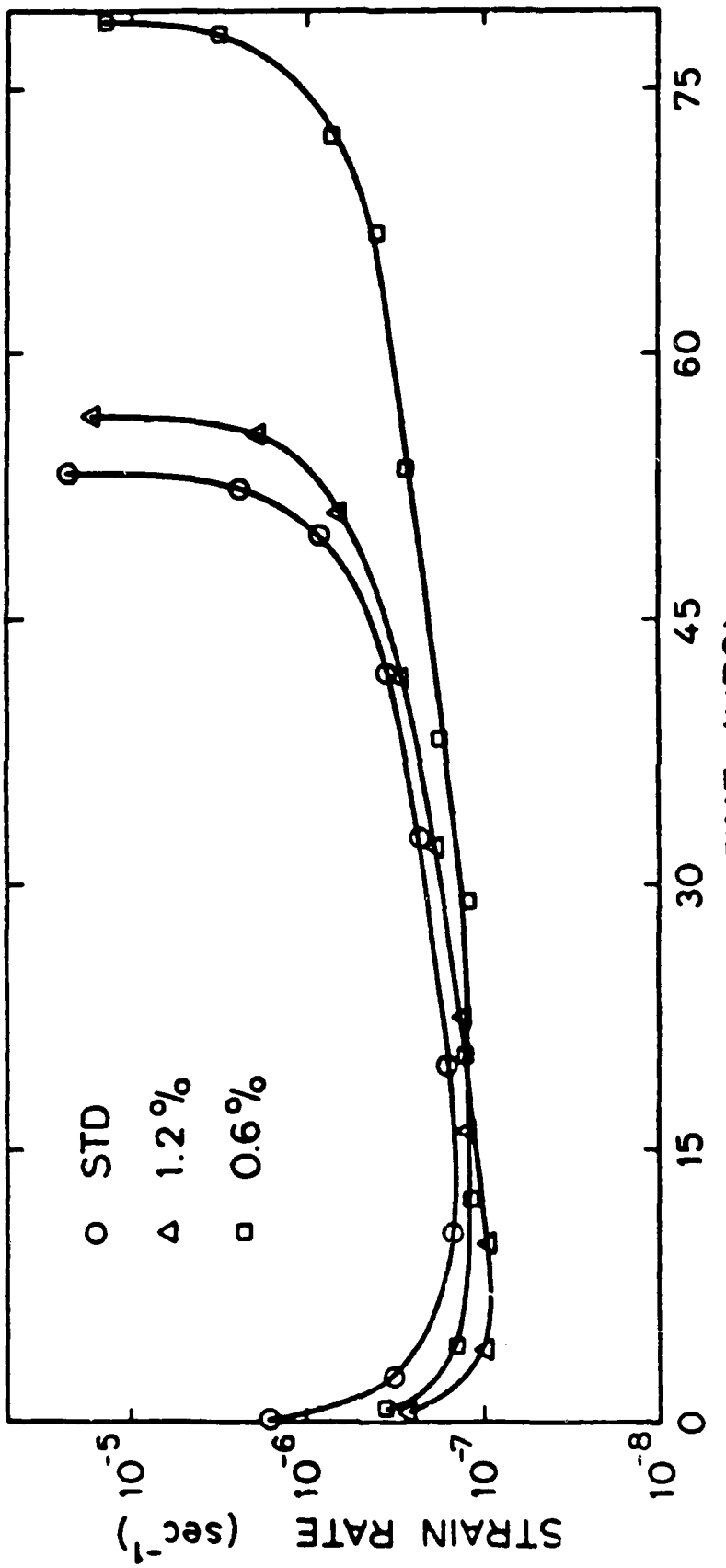

Fig. 6. Strain rate versus time for (○) standard, (□) 0.6 pct, and (△) 1.2 pct prestrained specimens of MA 754.

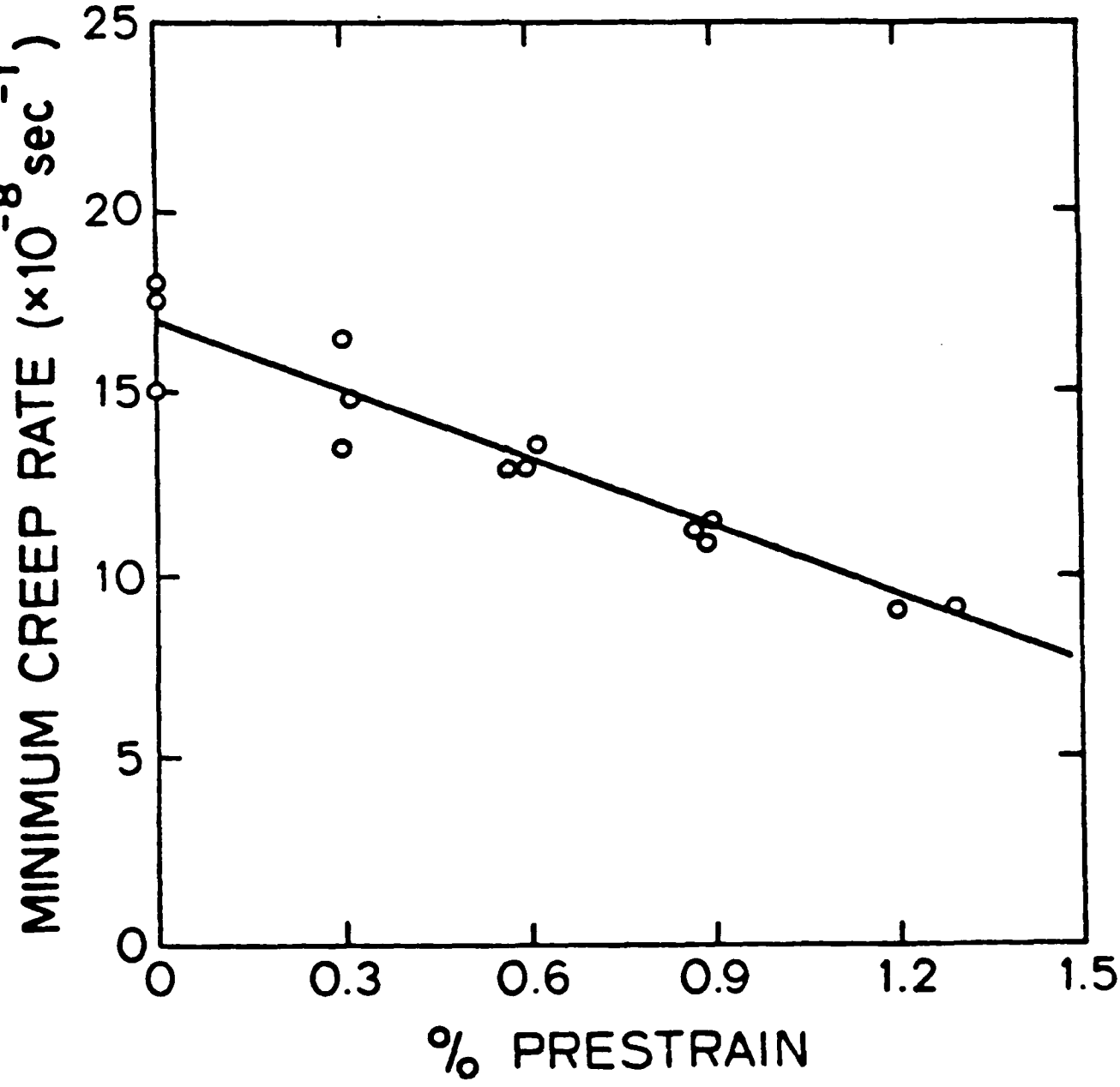

Fig. 7. Minimum creep rate at 224 MPa versus amount of prestrain at 276 MPa.

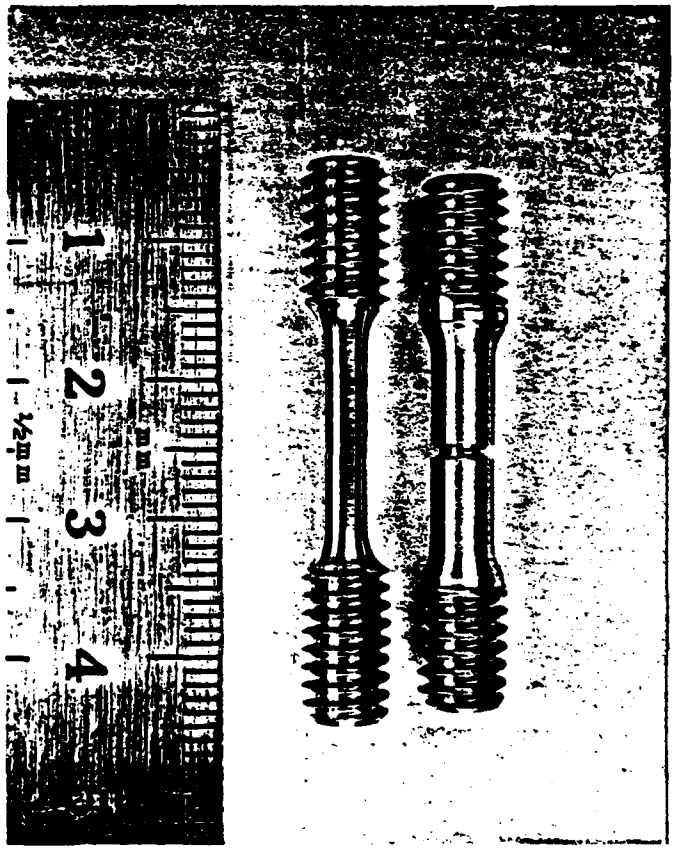

Fig. 8. Circumferentially notched specimen with an elastic stress concentration factor of 3.

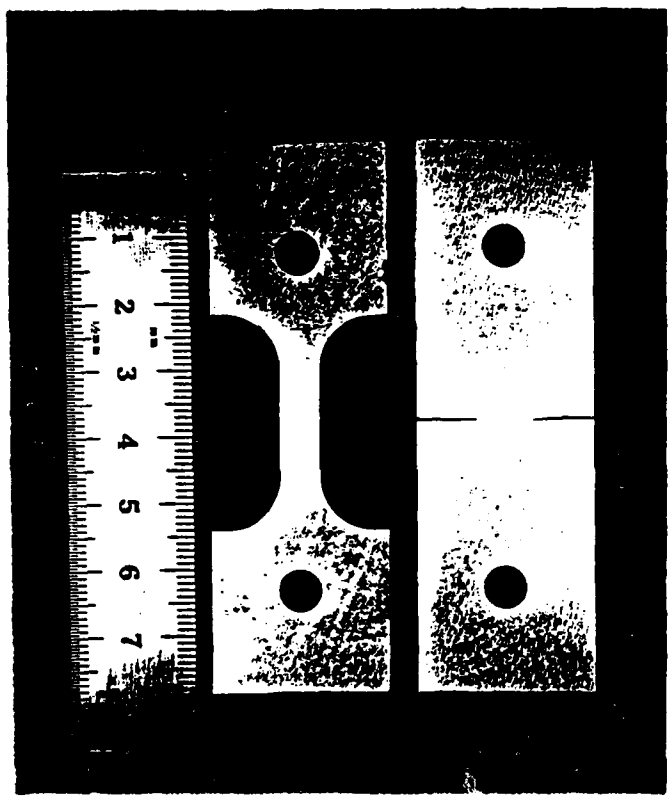

Fig. 9. Flat specimen notched on opposite sides of the gage section with an elastic stress concentration factor of 10.

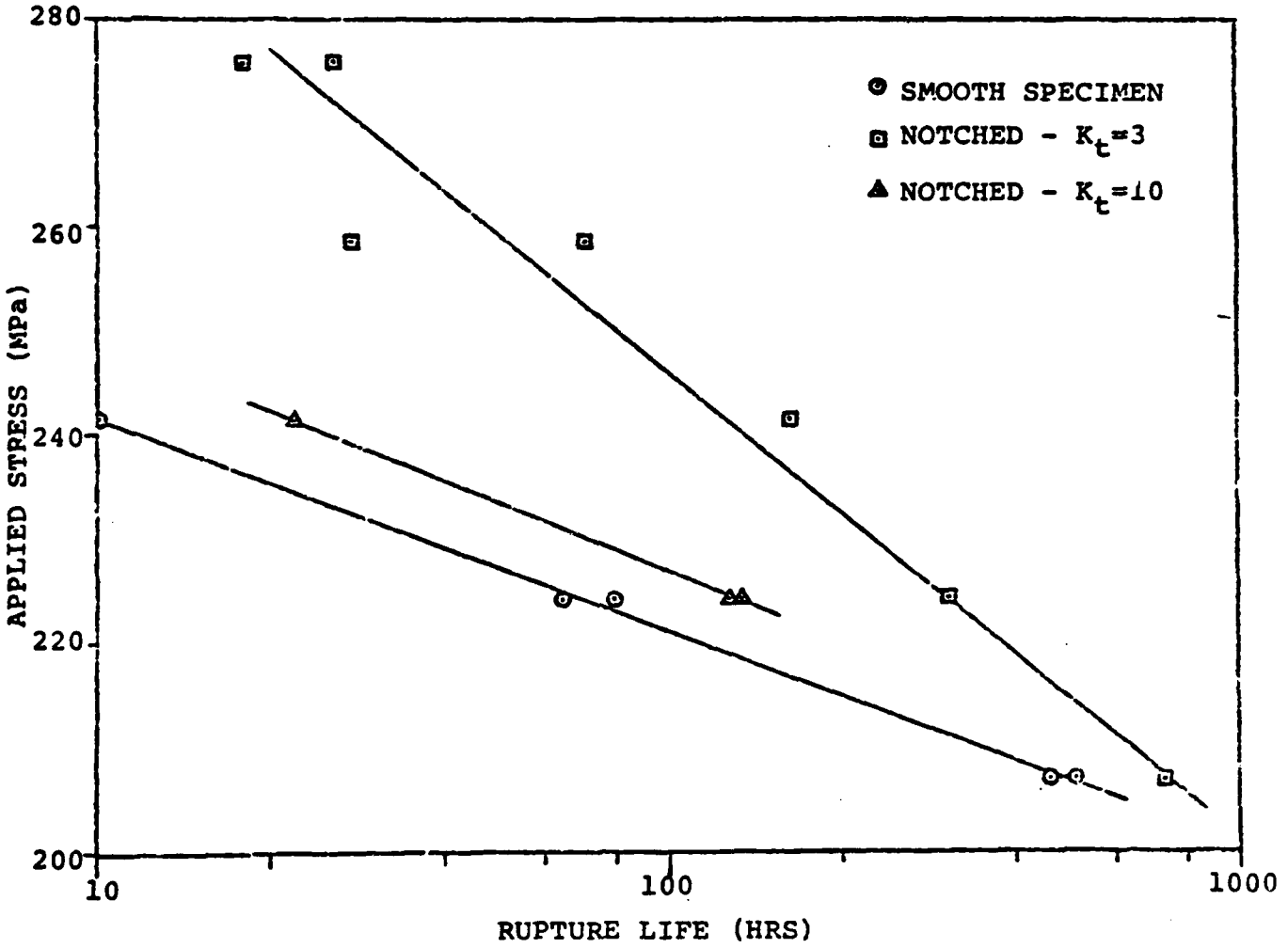

Fig. 10. Applied stress versus rupture life for MA 754 at 760°C-smooth reference, notched K_t = 3, and notched K_t = 10 specimens.

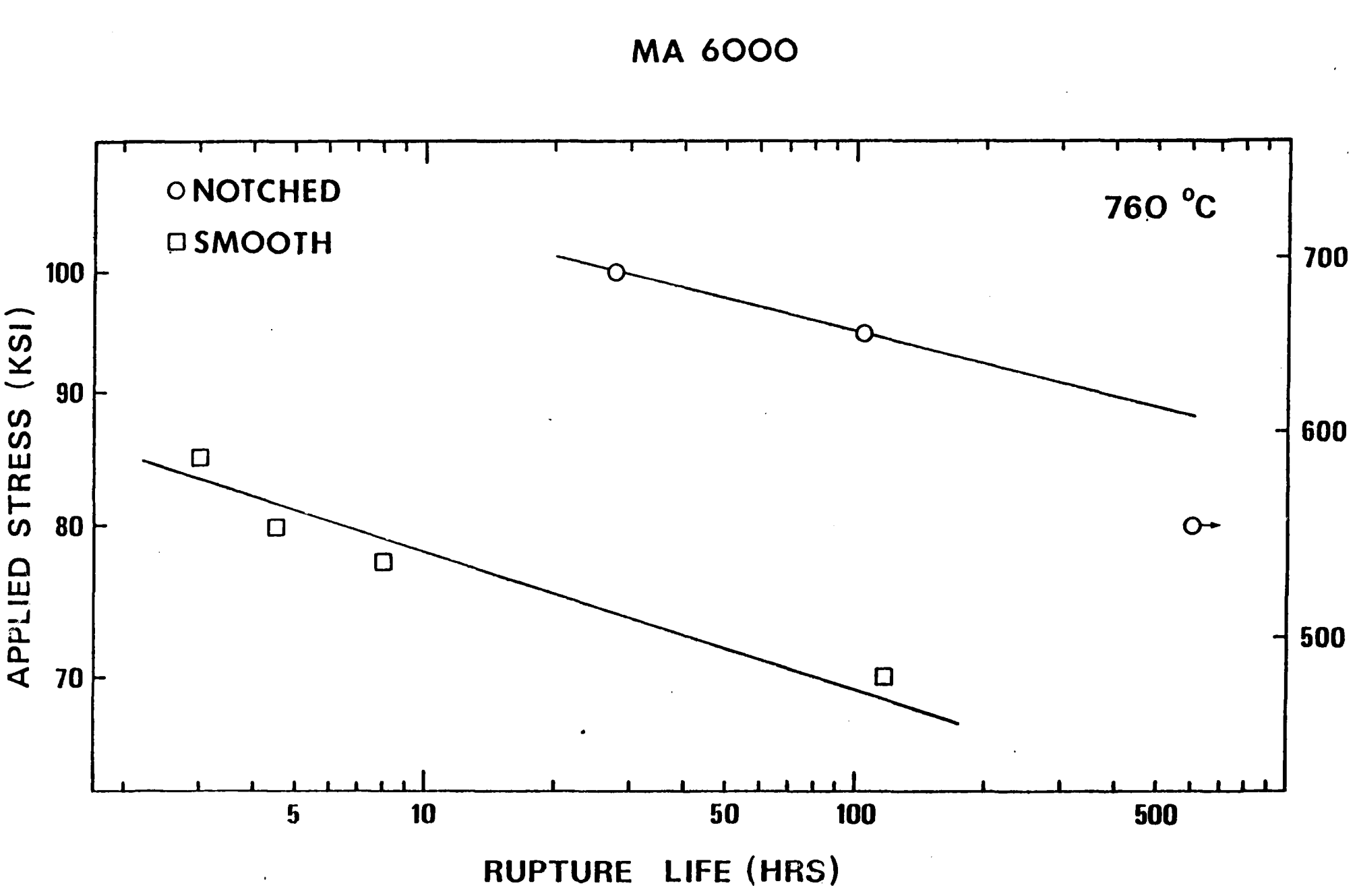

Fig. 11. Applied stress versus rupture life for MA 6000 at 760°C-smooth reference and notched K_t = 3.

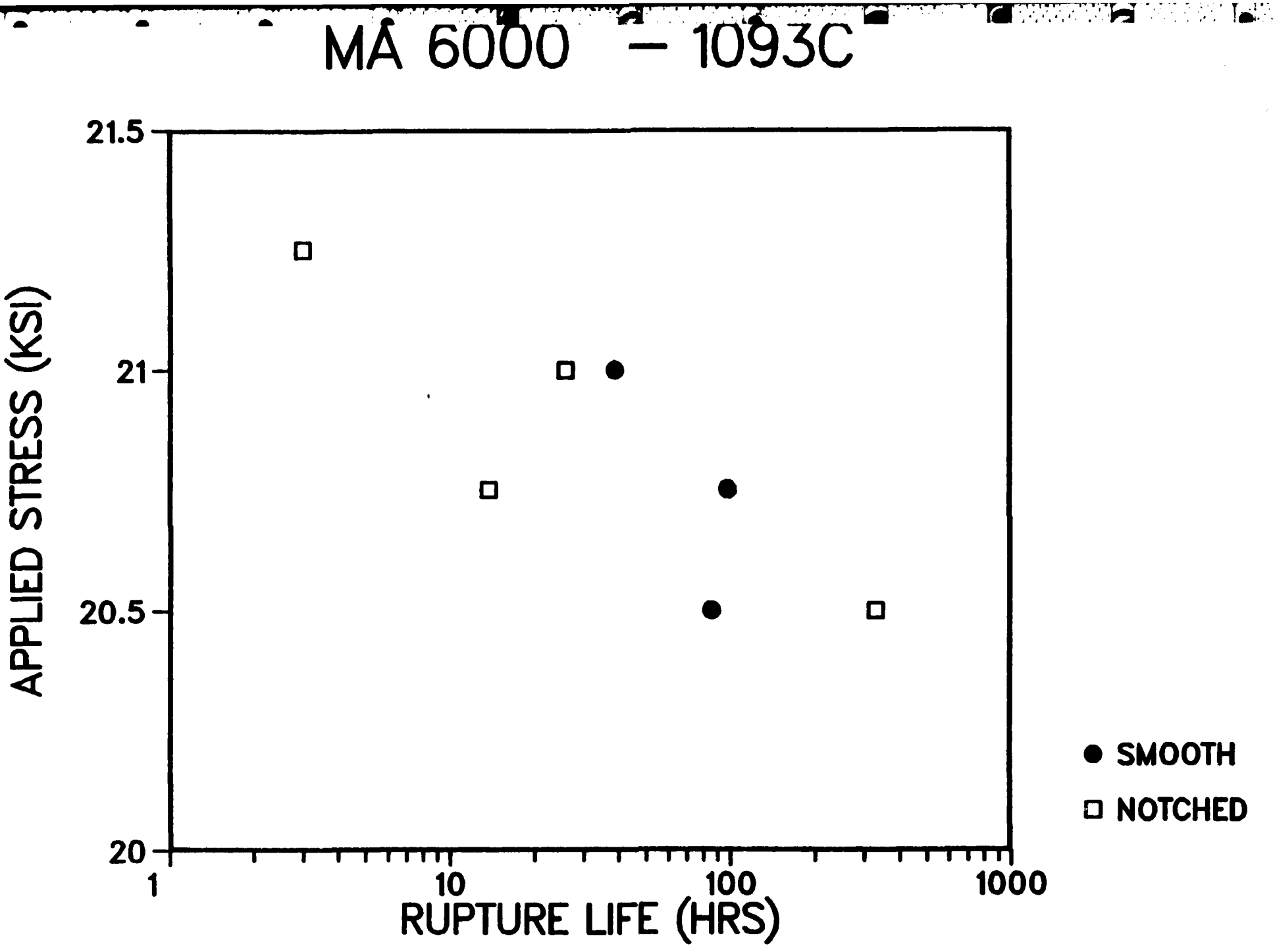

Fig. 12. Applied stress versus rupture life for MA 6000 at 1093°C-smooth reference and notched K_t = 3.

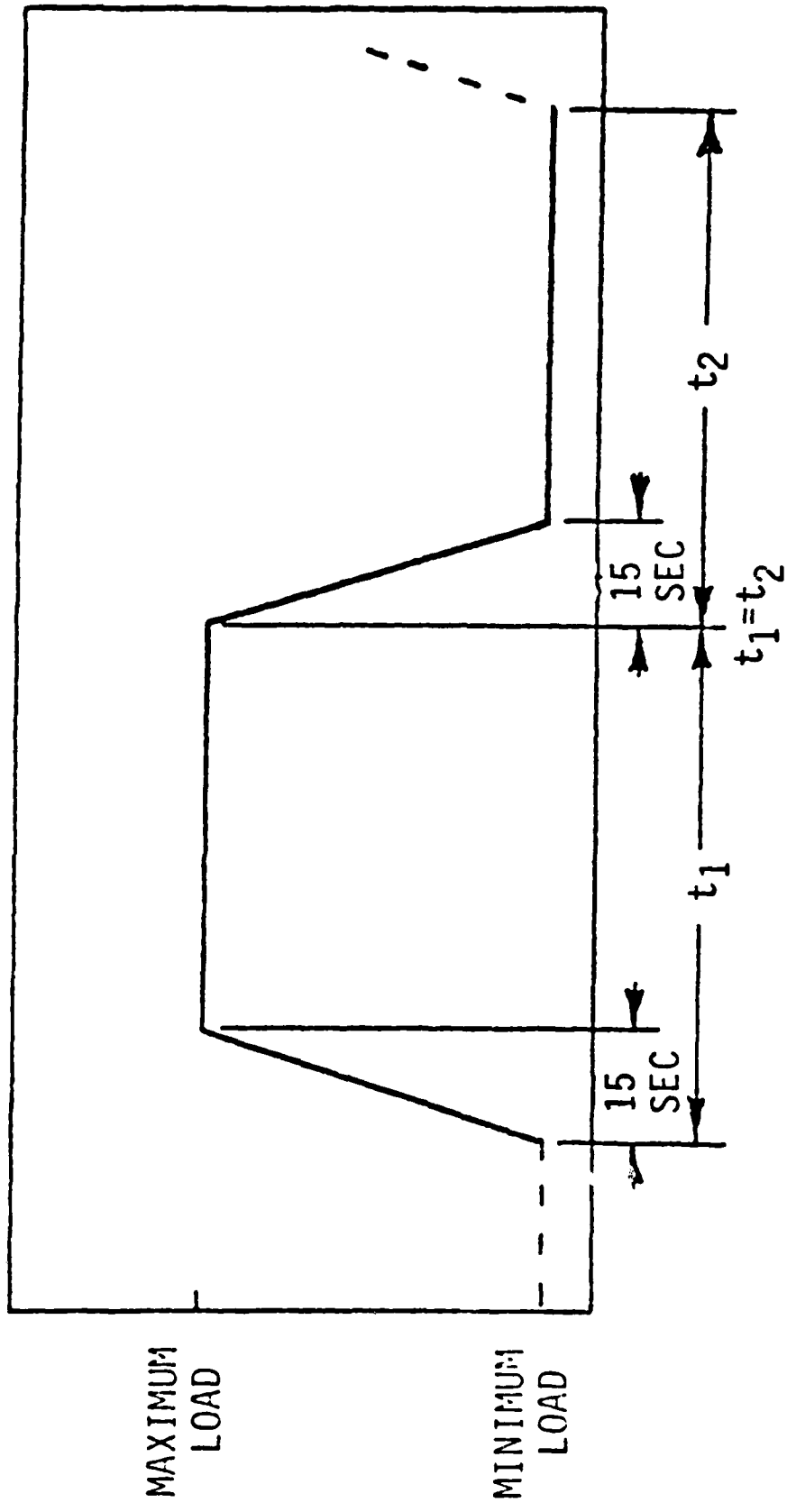

Fig. 13. Schematic representation of a single load cycle during cyclic creep testing.

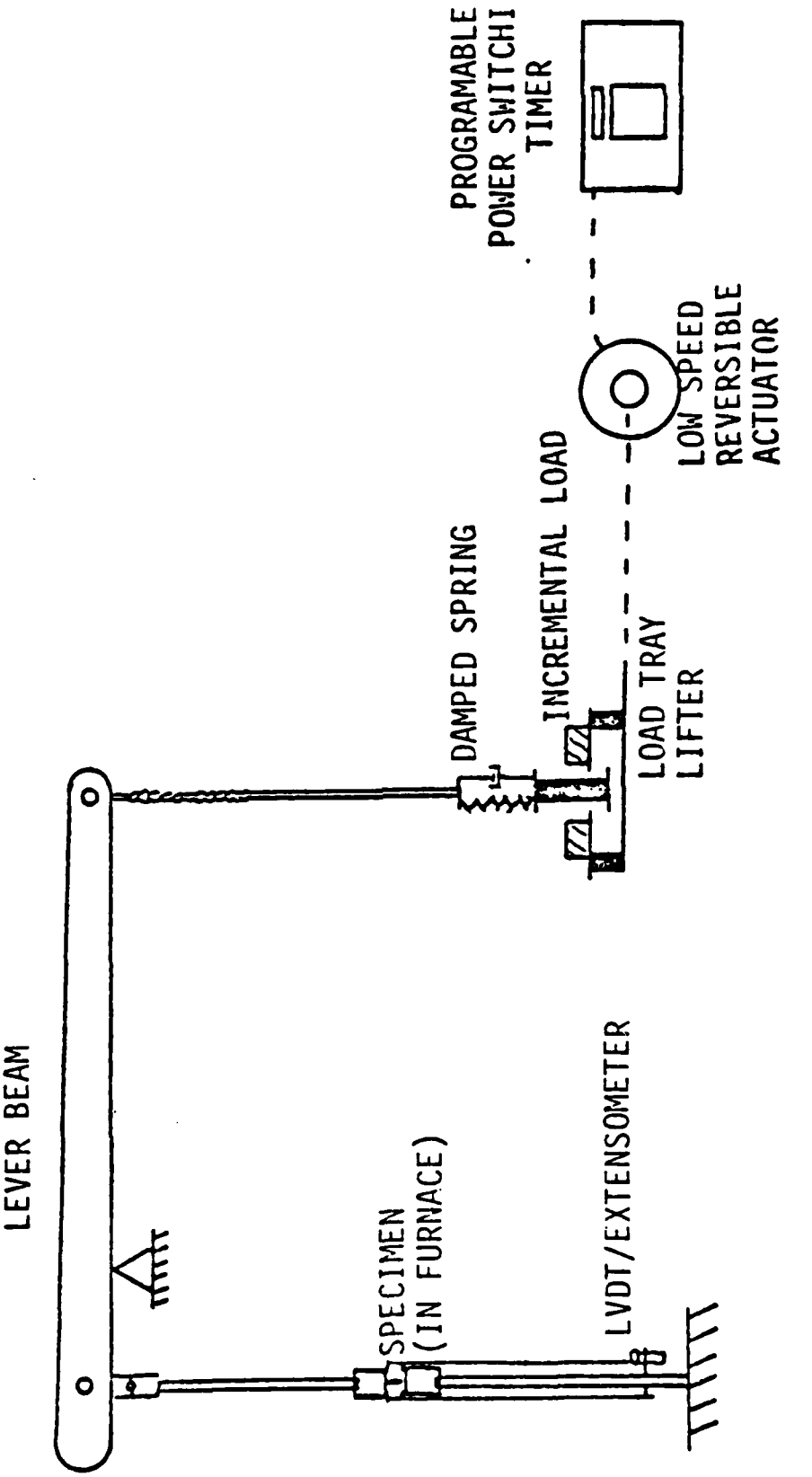

Fig. 14. Schematic diagram of the cyclic creep testing system.

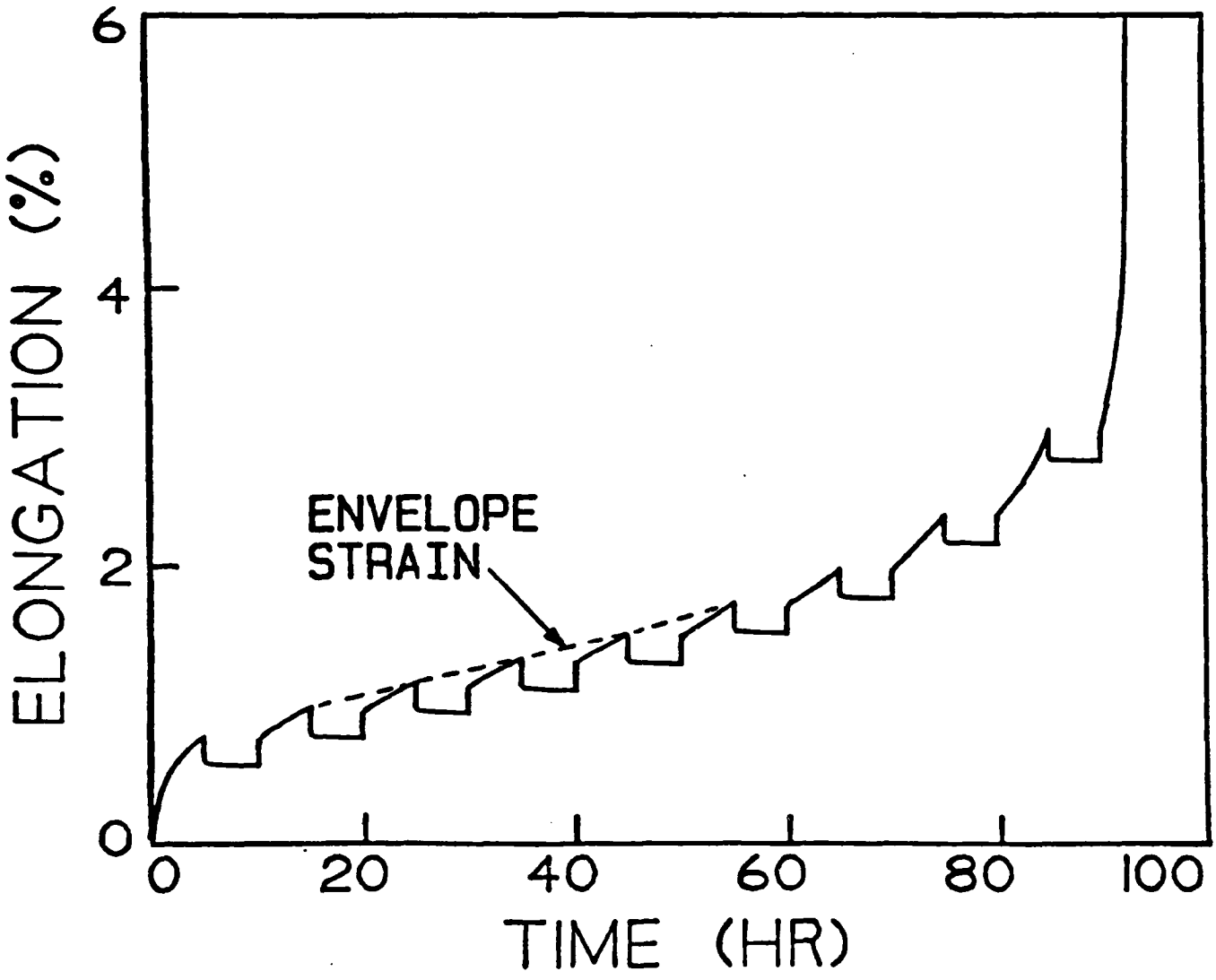

Fig. 15. Strain versus time for an entire cyclic creep test of MA 754; cyclic frequency 0.1 hr^{-1}, load 221-41 MPa.

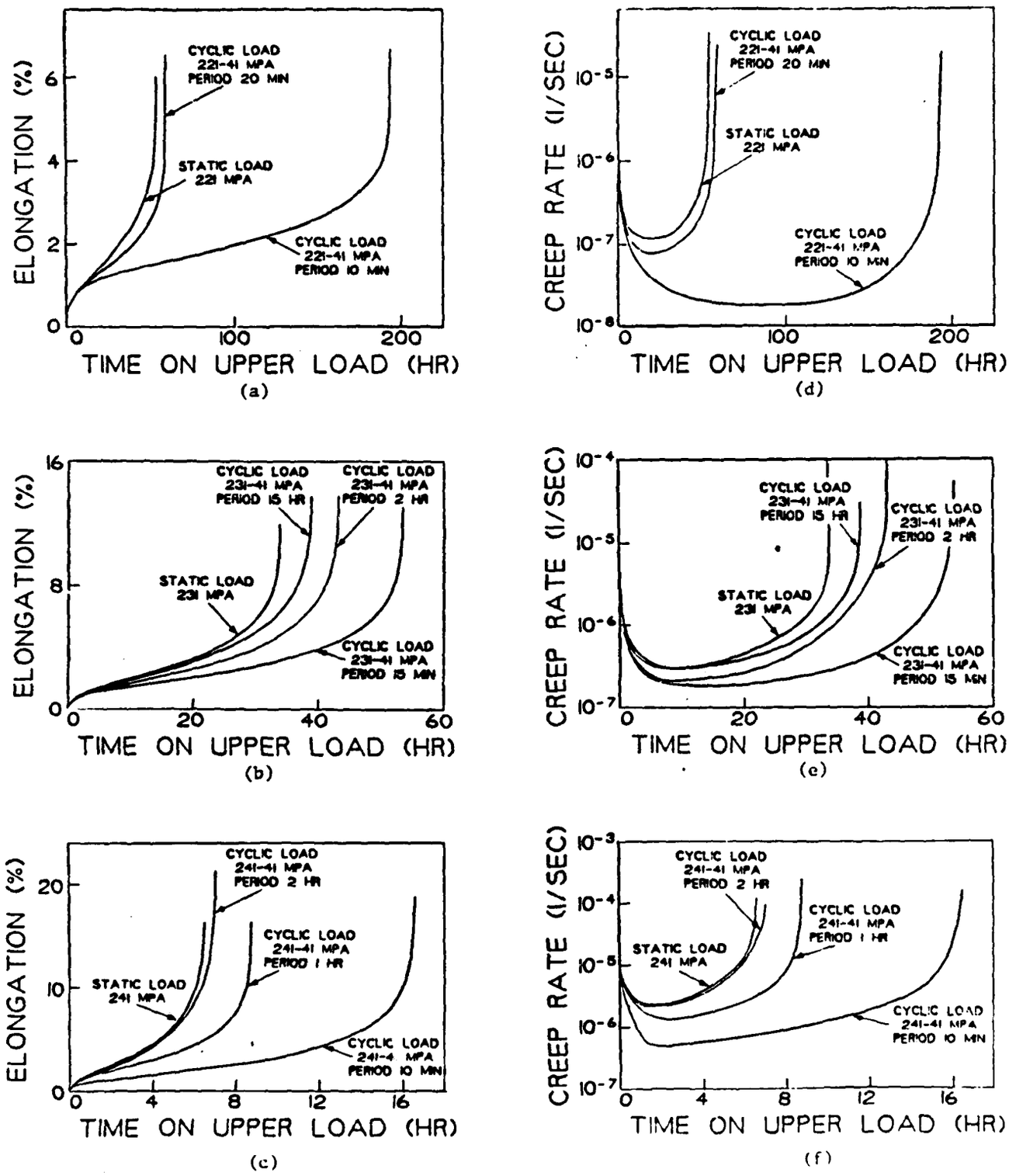

Fig. 16. (a-c) Envelope strain versus time on load for the range of cyclic loads and cyclic frequencies for MA 754; (d-f) Envelope strain rate versus time on load for the same tests.

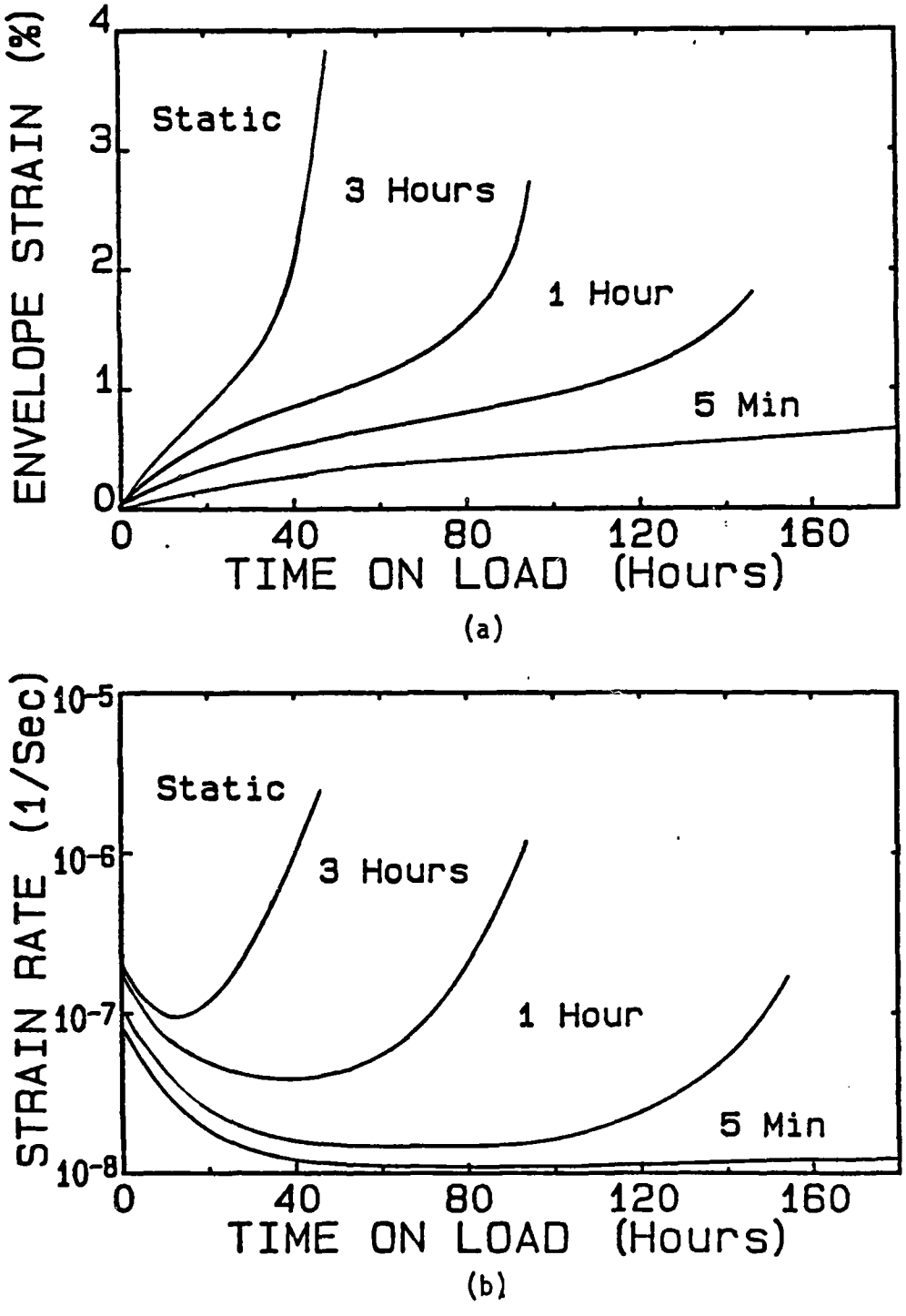

Fig. 17. (a) A static and three cyclic creep curves for MA 6000 with hold times of 3 hours, 1 hour, and 5 minutes. (b) A differential plot of 5(a) represented as the log of the strain rate versus time on load.

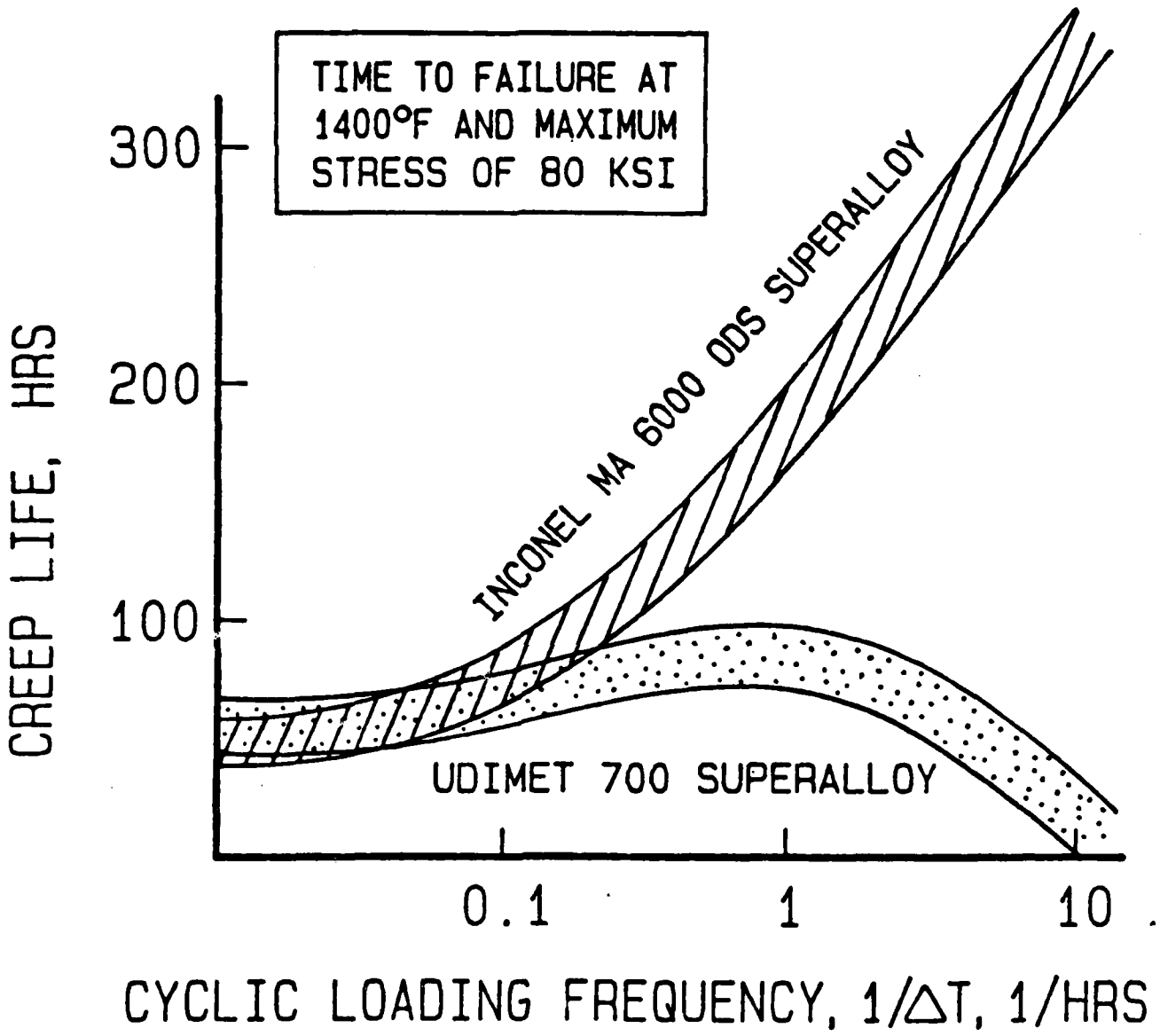

Fig. 18. Rupture life versus cyclic frequency for MA 6000 and Udimet 700, a conventional superalloy.

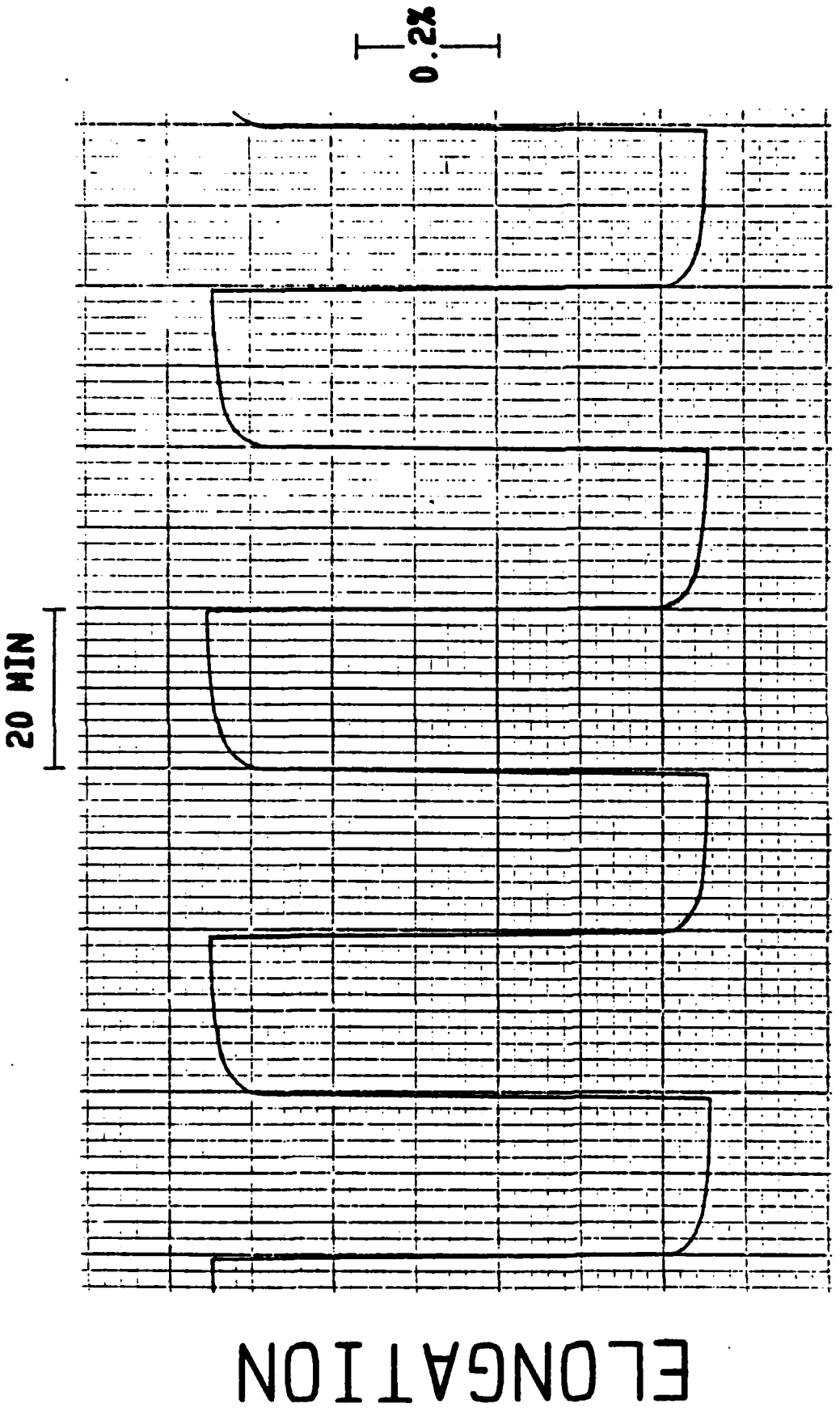

Fig. 19. Copy of typical data for MA 6000 taken by a chart recorder connected to a LVDT for a test with a period of 40 minutes.

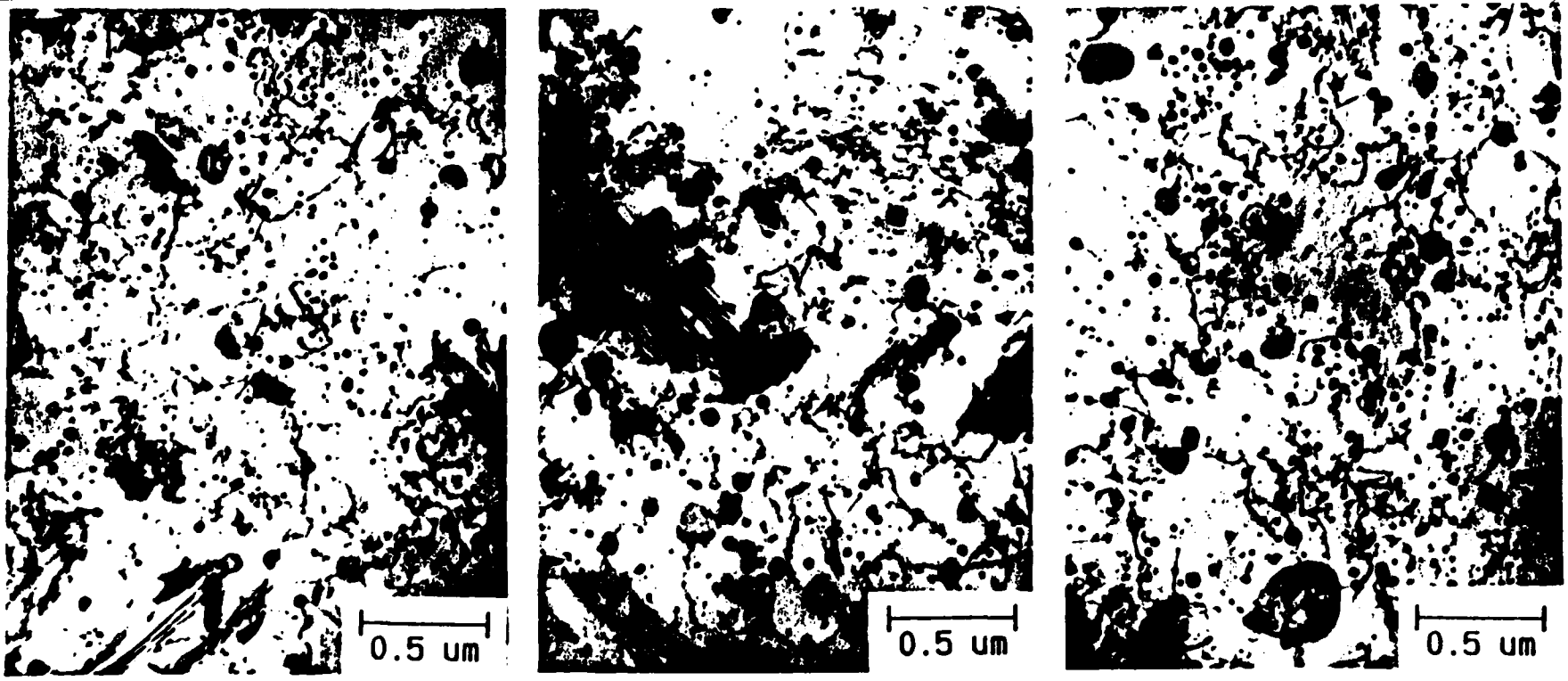

Fig. 20. TEM dislocation microstructures for test specimens of MA 754 interrupted at 1.5 pct strain for (a) 221 MPa static load, (b) 221.41 MPa cyclic load at 0.5 cycles/hour, and (c) 221.41 MPa cyclic load at 6 cycles/hour.

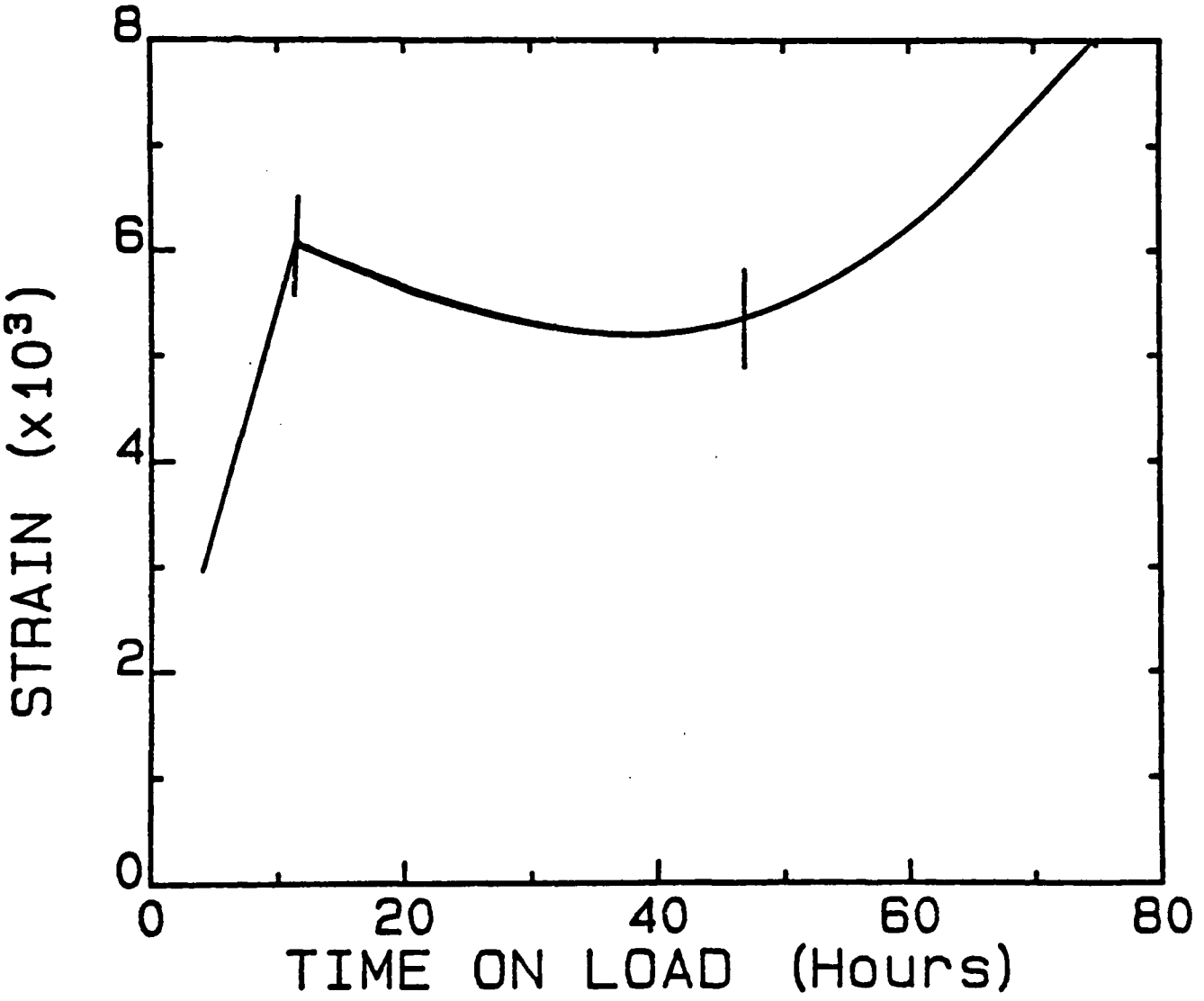

Fig. 21. Strain versus time on load for the mixed mode test of MA 6000 ; the marks indicate when the change in the mode of load application occurred.

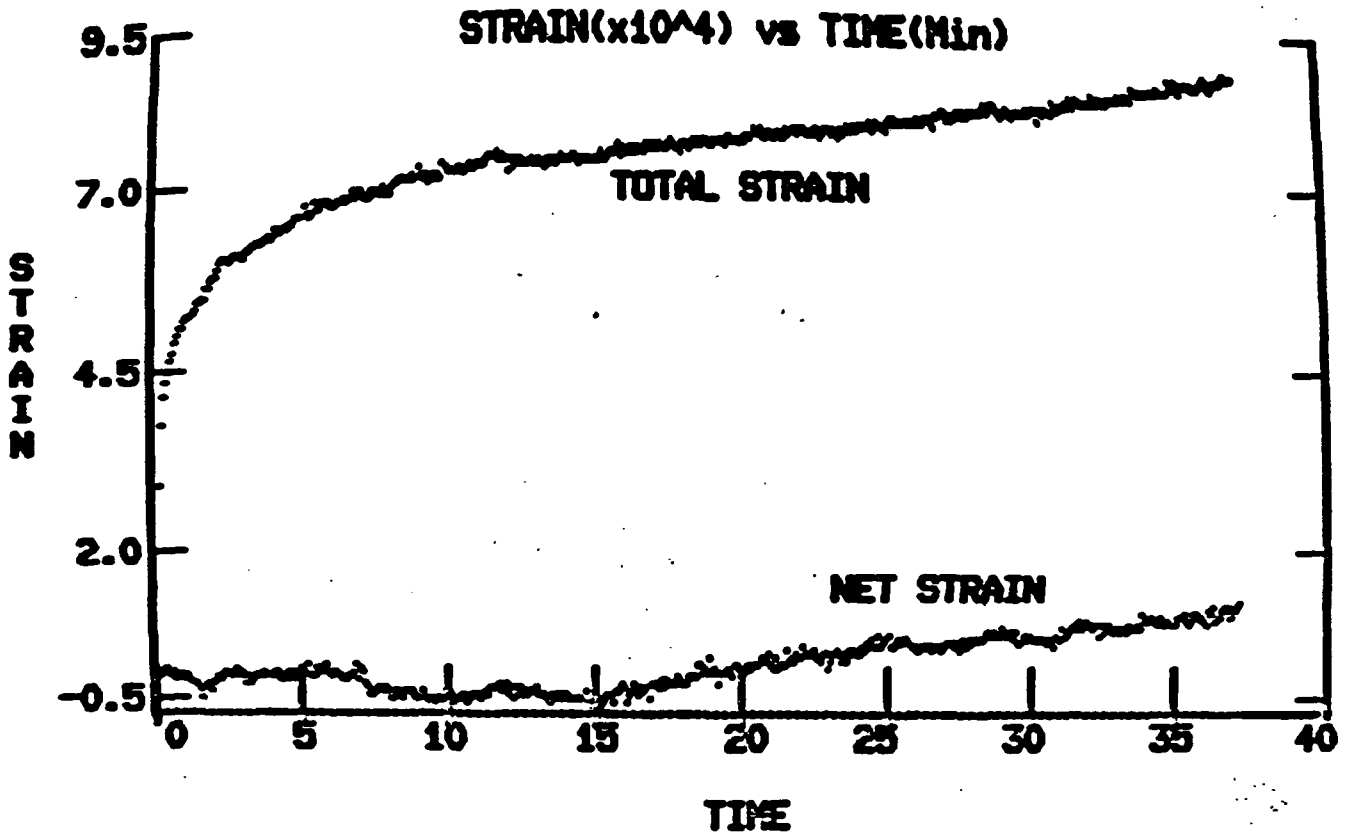

Fig. 22. The upper curve is the total strain on load versus time. The lower curve is a point by point subtraction of the total strain on load (versus time) less the anelastic strain (versus time) of the previous cycle, defined here as net strain. These results are for MA 6000 test with a period of two hours.

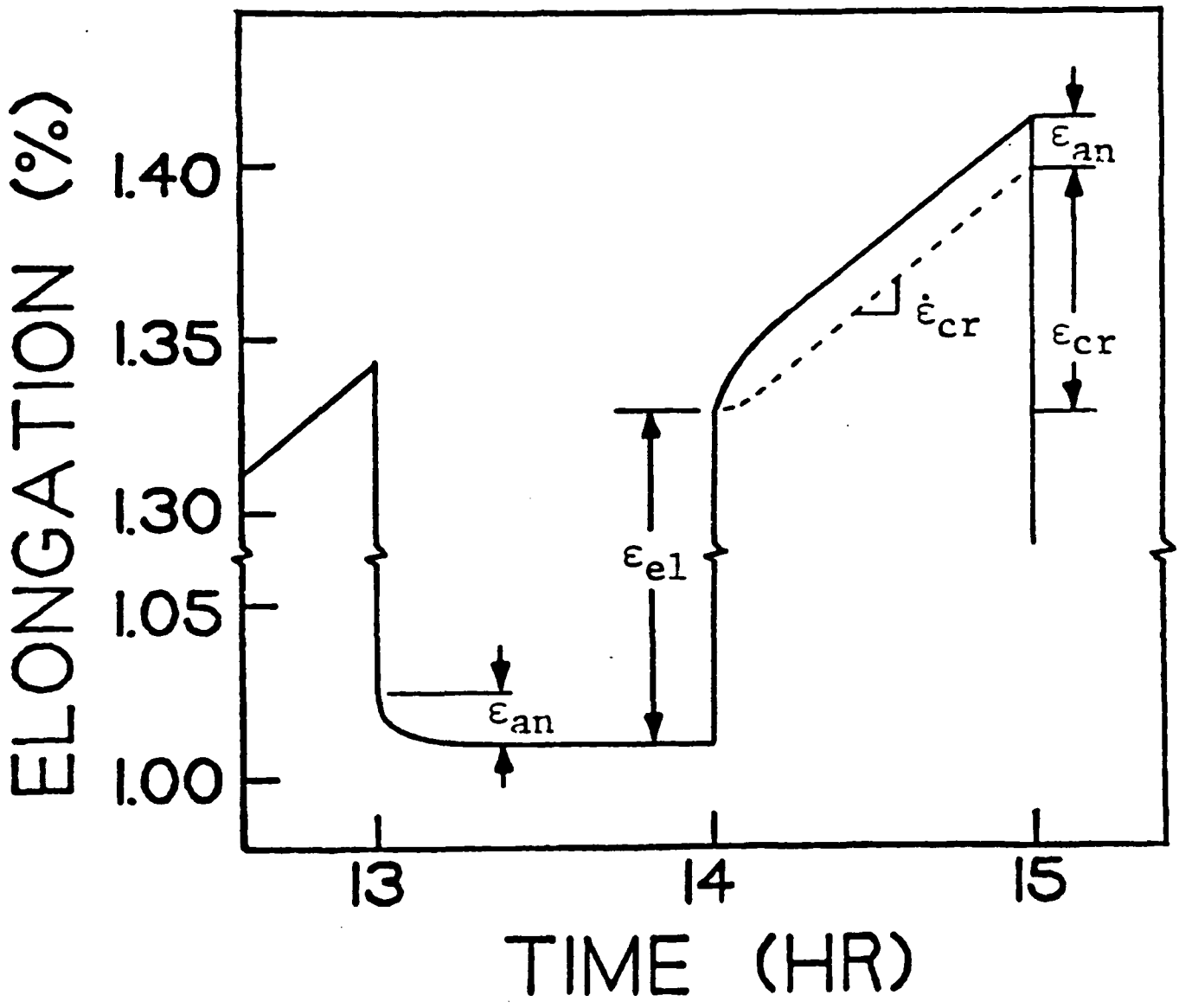

Fig. 23. Strain versus time for one cycle of the MA 754 cycle creep test at 0.5 cycles per hour and 221.41 MPa.

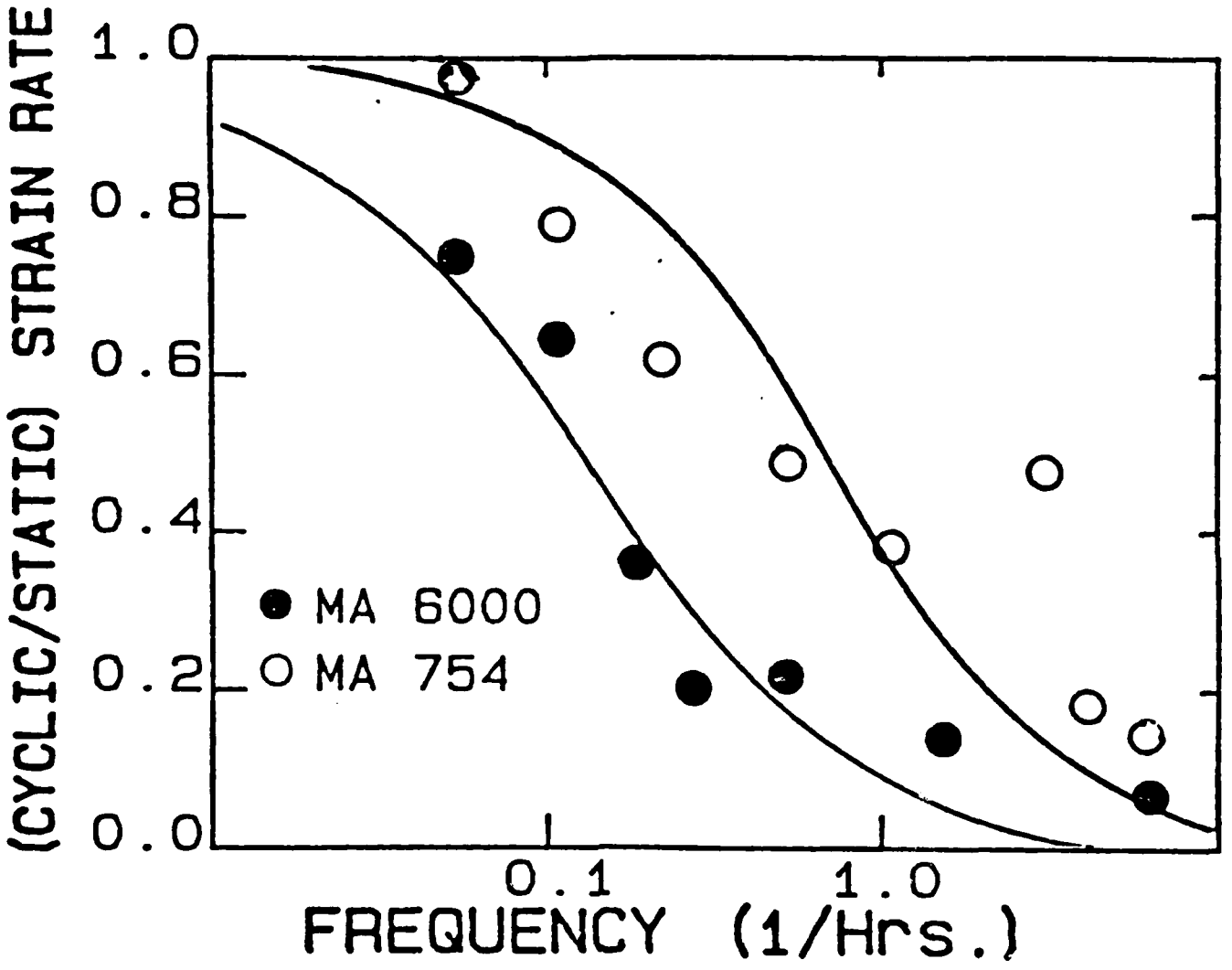

Fig. 24. Ratio of the cyclic to static strain rate versus frequency for MA 754 and MA 6000 . The line is derived from Equation (3) with the best fit value being chosen for t*.

TABLE I.

MA 754 CREEP DATA

	MINIMUM CREEP RATE ($x10^{-8}$ sec^{-1})	STRAIN TO ONSET OF TERTIARY (%)	STRAIN TO RUPTURE (%)	TIME TO ONSET OF TERTIARY (HRS)	TIME TO RUPTURE (HRS)	TIME SPENT IN TERTIARY (HRS)
206.8 MPa						
STANDARD	1.17	1.6	6.4	220	464.8	244.8
STANDARD	1.74	2.4	8.2	300	517.4	217.4
HIP-1177	*1.07*	*2.0*	*5.6*	*420*	*725.0*	*305.0*
224.1 MPa						
STANDARD	12.3	2.4	12.0	45	81.5	36.5
STANDARD	11.9	2.2	7.0	39	64.7	25.7
HIP-1177	*8.42*	*2.5*	*10.8*	*65*	*114.7*	*49.7*
241.3 MPa						
STANDARD	139	3.0	14.3	4.5	9.8	5.3
STANDARD	121	2.5	13.8	5.3	10.3	5.0
HIP-1177	*87.7*	*3.1*	*17.2*	*6.0*	*15.4*	*9.4*

Table II. Static and Cyclic Creep and Rupture Data of Inconel MA 754

Testing mode and applied stress (MPa)		Cyclic period	Creep rate†	Rupture life† (hrs)		Elongation at rupture (%)		Cycles to failure	
				Part I†† of bar	Part II of bar	Part I of bar	Part II of bar	Part I of bar	Part II of bar
Static creep	221		Ave. 1.58×10^{-7}	Ave. 54		Ave. 7.6		1	
	231		Ave. 3.16×10^{-7}	Ave. 34		Ave. 13.2		1	
	241		2.51×10^{-6}	6.5		16.4		1	
Cyclic creep	221-41	10 min	2.51×10^{-8}	194		6.9		2328	
	221-41	15 min	3.16×10^{-8}		390		12.1		3120
	221-41	20 min	7.94×10^{-8}	59		6.6		354	
	221-41	40 min	6.66×10^{-8}	83		7.2		247	
	221-41	1 hr	6.31×10^{-8}		153		11.3		306
	221-41	2 hr	7.94×10^{-8}	58		3.8		58	
	221-41	5 hr	1.00×10^{-7}		158		14.4		63
	221-41	10 hr	1.26×10^{-7}	48		6.0		10	
	221-41	20 hr	1.58×10^{-7}		125		9.0		12
	231-41	15 min	2.00×10^{-7}	54		13.1		432	
	231-41	2 hr	2.51×10^{-7}	43		13.9		43	
	231-41	15 hr	3.16×10^{-7}	39		13.8		5	
	241-41	10 min	5.01×10^{-7}	17		18.7		204	
	241-41	1 hr	1.58×10^{-6}	9		16.4		18	
	241-41	2 hr	2.51×10^{-6}	7		21.4		7	

Table III

Cyclic Creep Strain Rate and Rupture Life Data for MA 6000

CYCLIC PERIOD	CREEP RATE x 10^{-8}/sec	RUPTURE LIFE
Static	9.55	44 hrs
20 hrs	7.24	49 hrs
10 hrs	6.31	65 hrs
6 hrs	3.53	94 hrs
4 hrs	2.04	151 hrs
2 hrs	2.19	149 hrs
40 min	1.45	---
10 min	0.81	---

List of Publications and Presentations

The following publications and presentations have resulted wholly or in part from the AFOSR grant-funded research.

Publications

1. "On the Concept of Back Stress in Particle Strengthened Alloys," S. Purushothaman, O. Ajaja and J.K. Tien, in Strength of Metals and Alloys, Vol. 1, ICSMA5, P. Haasen, V. Gerold and G. Kostorz, eds., Pergammon Press, 1979.
2. "The Role of the Alloy Matrix in the Creep Behavior of Particle-Strengthened Alloys," O. Ajaja, T.E. Howson, S. Purushothaman and J.K. Tien, Mats. Sci. Eng. 44, 165 (1980).
3. "Creep Deformation and Rupture of Oxide Dispersion Strengthened Inconel MA 754 and MA 6000E," T.E. Howson, F. Cosandey and J.K. Tien, in Superalloys 1980, Proceedings of the Fourth International Symposium on Superalloys, J.K. Tien, S.T. Wlodek, H. Morrow III, M. Gell and G.E. Maurer, eds., ASM Press, 1980.
4. "The Effect of Predeformation on the Creep and Stress Rupture of an Oxide Dispersion Strengthened Mechanical Alloy," R.T. Marlin, F. Cosandey and J.K. Tien, Met. Trans. A 11A, 1771 (1980).
5. "Anelastic Relaxation, Cyclic Creep and Stress Rupture of γ' and Oxide Dispersion Strengthened Superalloys," J.K. Tien, D.E. Matejczyk, Y. Zhuang and T.E. Howson, Creep and Fracture of Engineering Materials and Structures, B. Wilshire and D.R.J. Owen, eds., Pineridge Press, Swansea, U.K., 1981.
6. "Static and Cyclic Creep and Stress Rupture of Oxide Dispersion Strengthened Nickel-Base Alloys," J.K. Tien, T.E. Howson and D.E. Matejczyk, to be published in Proc. INCO Conf. on Frontiers of High Temperature Materials, New York, May 1981.

7. "Anelastic Relaxation Controlled Cyclic Creep and Cyclic Stress Rupture Behavior of an Oxide Dispersion Strengthened Alloy," D.E. Matejczyk, Y. Zhuang and J.K. Tien, Met. Trans. A, to be published February 1983.
8. "Cyclic Creep and Stress Rupture of a Mechanically Alloyed Oxide Dispersion and Precipitation Strengthened Nickel-Base Superalloy," V.C. Nardone, D.E. Matejczyk and J.K. Tien, Met. Trans. A, in press.

Presentations

1. "Effect of HIP Treatment on the Creep Behavior of MA 754," T.E. Howson and J.K. Tien, 108th Annual Meeting of AIME, New Orleans, February 1979.
2. "Notch Sensitive Stress Rupture Behavior of ODS Mechanical Alloy MA 754," F. Nami, D. Matejczyk and J.K. Tien, 108th Annual Meeting of AIME, New Orleans, February 1979.
3. "On the Concept of Back Stress in Particle Strengthened Alloys," T.E. Howson, S. Purushothaman, O. Ajaja and J.K. Tien, Fifth International Conference on the Strength of Metals and Alloys, Aachen, West Germany, August 1979.
4. "Creep and Stress Rupture of ODS and γ' Strengthened Engineering Alloys Under Cyclic Loading," D.E. Matejczyk, T.E. Howson and J.K. Tien, 109th Annual Meeting of AIME, Las Vegas, February 1980.
5. "Predeformation, Localized Deformation, and HIP Effects on Defects and Properties in MA 754," T.E. Howson, F. Cosandey and J.K. Tien, 109th Annual Meeting of AIME, Las Vegas, February 1980.
6. "Effects of Hot Isostatic Pressing on the Structure of an Oxide Dispersion Strengthened Alloy," A. Koren, F. Cosandey, T.K. Glasgow and J.K. Tien, 109th Annual Meeting of AIME, Las Vegas, February 1980.
7. "Effects of Higher Strain Rate Deformation on Structure and Creep Properties of an ODS Alloy," R.T. Marlin, F. Cosandey and J.K. Tien, 109th Annual Meeting of AIME, Las Vegas, February 1980.

8. "Creep and Stress Rupture Behavior of a Nickel-Base Superalloy Under Cyclic Loading," D.E. Matejczyk, Y. Zhuang and J.K. Tien, TMS-AIME Fall Meeting, Ocrober 1980.

9. "Cyclic Creep and Stress Rupture Behavior of Nickel-Base ODS and γ' Strengthened Alloys," D.E. Matejczyk, Y. Zhuang and J.K. Tien, 110th Annual Meeting of AIME, Chicago, February 1981.

10. "Notch Sensitive Stress Rupture Behavior of an Oxide Dispersion Strengthened Superalloy," T.E. Howson and J.K. Tien, 110th Annual Meeting of AIME, Chicago, February 1981.

11. "Creep Fracture Processes in ODS Alloy MA 754," C.T. Yen, F. Cosandey, T.E. Howson and J.K. Tien, 110th Annual Meeting of AIME, Chicago, February 1981.

12. "Advances in P/M and ODS Superalloys," J.K. Tien and T.E. Howson, Invited Speaker, 1981 ASM Materials Science Seminar on Advances in Powder Technology, Louisville, KY, October 1981.

13. "Cyclic Creep and Stress Rupture of a Mechanically Alloyed Oxide Dispersion and Precipitation Strengthened Nickel-Base Superalloy," V.C. Nardone, D.E. Matejczyk and J.K. Tien, 111th Annual AIME Meeting, Dallas, February 1982.

Theses Arising from the Research

Fereydoon Nami, "Notch Sensitive Stress Rupture Behavior of ODS Mechanical Alloy MA 754," Master's Thesis, Columbia University, May 1979.

Avi Koren, "The Effect of HIP on the Creep Rupture Properties and the Microstructure of ODS Alloy MA 754," Master's Thesis, Columbia University, October 1979.

Robert Marlin, "The Effect of Predeformation on the Creep and Stress Rupture of an Oxide Dispersion Strengthened Mechanical Alloy," Master's Thesis, Columbia University, October 1979.

Yen Chin-Tang, "Mechanisms of Stress Rupture in the ODS Alloy MA 754," Master's Thesis, Columbia University, September 1981.

Mona McAlarney, "Creep and Stress Rupture of Oxide Dispersion Strengthened Alloys and Superalloys," Master's Thesis, Columbia University, November 1981.

Dan Matejczyk, "Elevated Temperature Cyclic Creep and Cyclic Stress Rupture of Particle Strengthened Alloys," Engineering Science Doctoral Thesis, Columbia University, expected 1983.

Vince Nardone, "Cyclic Creep and Stress Rupture of an ODS Superalloy," Master's Thesis, Columbia University, May 1982.

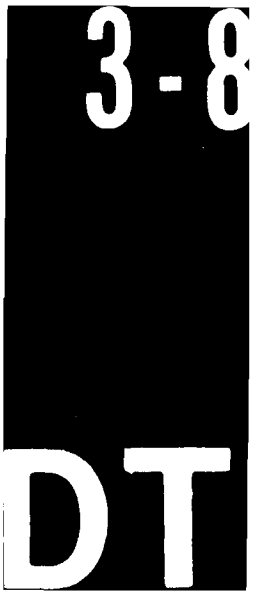
3-8
DT